



# Comparison of the NASA Common Research Model European Transonic Wind Tunnel Test Data to NASA Test Data (Invited)

Melissa B. Rivers<sup>1</sup>

*NASA Langley Research Center, Mail Stop 267, Hampton, VA 23681*

Jürgen Quest<sup>2</sup>

*ETW, European Transonic Wind tunnel, D-51147, Cologne, Germany*

Ralf Rudnik<sup>3</sup>

*DLR, German Aerospace Center, 38108 Braunschweig, Germany*

**Experimental aerodynamic investigations of the NASA Common Research Model have been conducted in the NASA Langley National Transonic Facility, the NASA Ames 11-ft wind tunnel, and the European Transonic Wind Tunnel. In the NASA Ames 11-ft wind tunnel, data have been obtained at only a chord Reynolds number of 5 million for a wing/body/tail = 0 degree incidence configuration. Data have been obtained at chord Reynolds numbers of 5, 19.8 and 30 million for the same configuration in the National Transonic Facility and in the European Transonic Facility. Force and moment, surface pressure, wing bending and twist, and surface flow visualization data were obtained in all three facilities but only the force and moment, surface pressure and wing bending and twist data are presented herein.**

## Nomenclature

$b$	=	wing span, in.
$c$	=	wing mean aerodynamic chord, in.
$C_D$	=	drag coefficient
$C_L$	=	lift coefficient
$C_m$	=	pitching moment coefficient referenced to 0.25 of the wing mean aerodynamic chord
$C_p$	=	pressure coefficient
CRM	=	Common Research Model
DPW	=	Drag Prediction Workshop
$E$	=	modulus of elasticity
ESWIRP	=	European Strategic Wind Tunnels Improved Research Potential
$M_\infty$	=	freestream Mach number
NTF	=	National Transonic Facility
$p_t$	=	total pressure, psi
$q_\infty$	=	dynamic pressure, psf

<sup>1</sup> Research Engineer, Configuration Aerodynamics Branch, Mail Stop 267, Senior Member AIAA

<sup>2</sup> Chief Aerodynamicist, European Transonic Wind Tunnel, Ernst-Mach Strasse, D-51147 Cologne, Germany, Associate Fellow AIAA

<sup>3</sup> Head Transport Aircraft, Institute of Aerodynamics and Flow Technology, Lilienthalplatz 7, 38112 Braunschweig, Germany, Member AIAA

$Re_c$	=	Reynolds number based on mean aerodynamic chord
$S$	=	model reference area, $ft^2$
$T_t$	=	Total temperature, $^{\circ}F$
WBT0	=	Wing/Body/Tail= $0^{\circ}$
$x/c$	=	longitudinal distance from wing leading edge nondimensionalized by local wing chord
$\alpha$	=	angle of attack, degree
$\eta$	=	fraction of wing semi-span

## I. Introduction

The NASA Common Research Model (CRM) serves as a backbone for providing wind tunnel data for code validation and verification for transonic commercial aircraft. The model has been designed and built as part of the AIAA drag prediction workshop (DPW) introduced with the DPW IV.

The latest use of the model in the European Transonic Wind Tunnel (ETW) is embedded in the framework of the European project ESWIRP (European Strategic Wind Tunnels Improved Research Potential). This so-called infrastructure project is part of the 7th framework program. The objective has been to improve the capabilities of selected strategic wind tunnel facilities in Europe, and, at the same time, to provide efficient access to these facilities to academia and research establishments for selected research projects addressing fundamental aerodynamic topics. The focus for the use of the ETW is on improving unsteady testing capabilities for exploring limits of the flight envelope. For this purpose, an international consortium has been formed under the coordination of ONERA consisting of the University of Stuttgart and the German Aerospace Center, DLR (Germany), the Federal State Unitary Enterprise Central Aerohydrodynamic Institute, TSAGi (Russia), the Academy of Sciences (Czech Republic), the Aerospace Research and Test Establishment VZLU (Czech Republic), and the Von Karman Institute for fluid Dynamics (Belgium). The consortium submitted a scientific proposal entitled “Time-Resolved Wake Measurements of Separated Wing Flow & Wall Interference Investigations”, which has been evaluated and selected for realization by an expert panel in 2012. The proposal addresses unsteady wake interference effects between the wake of an aircraft wing and the horizontal tail plane. Due to the international character of the study and the intention to provide test data to the general public, NASA’s CRM, representing a typical commercial aircraft configuration appears to be an ideal candidate to serve as a wind tunnel model for the experimental investigations as it is also suited for cryogenic testing. Based on a bilateral agreement between NASA and DLR, the model has been provided by NASA, while it is introduced to the consortium by DLR. The overall project is described in reference 1.

The background of the experimental activities is the high-speed stall of transport aircraft at the boundaries of the flight envelope, which produces massively separated flow on the wing itself and in its wake. Unsteady oscillating of the separation point and large-scale turbulent fluctuations lead to strong unsteadiness of the wake flow. The relevance to investigate these aerodynamic effects is given by the fact that they bear the risk of exciting structural vibrations due to unsteady air loads in a certain frequency domain. Moreover, they influence the efficiency of control surfaces on the horizontal stabilizer and the elevator. In the case of asymmetry in some separation areas of the wing and the resulting wake, unsteady rolling moments may be excited and induced to the tail plane. These effects of flow unsteadiness at the tail plane can become critical and might require potential load alleviation systems at the tail plane. Thus, the knowledge of the formation, propagation, and impact of large-scale turbulent fluctuations are of interest for the design of commercial aircraft.

A key element to understanding these effects is time-resolved (TR) measurement in the wing wake. Such measurements, carried out by DLR with a special Particle Image Velocimetry System (PIV), are the main element of the ETW test in the current framework. The corresponding TR-PIV measurements under cryogenic conditions are described in reference 2. Complementary to these measurements, the test provides reference data on the wind tunnel walls to study wall interference effects and eventually improve wall correction methods.

The tests have been carried out on the wing/body/tail = 0 (WBT0) degree incidence configuration of the CRM for low and high speed conditions in the linear lift range up to the highest possible angles of attack. Complementary to the unsteady flow field measurements, classical aerodynamic parameters such as forces, moments, and wall pressure distributions have been recorded. These data are supplemented by wing deformation measurements as the test has been conducted in a low temperature and high-pressure environment to produce flight Reynolds number conditions.

The test matrix has been set-up such that a comparison of the ETW test data to existing data from the NASA’s NTF and the Ames 11ft wind tunnel is possible. The present contribution describes the classical experimental results

of the ETW test and compares the data to corresponding results of previous tests with the CRM in the aforementioned facilities.

## II. Experimental Approach

### A. Facility Description

#### 1. National Transonic Facility

The NTF<sup>3</sup> is a unique national facility (Figure 1) that enables testing of aircraft configurations at conditions ranging from subsonic to low supersonic speeds at Reynolds numbers up to full-scale flight values. The NTF is a conventional, closed circuit, continuous-flow, fan-driven, pressurized wind tunnel (Figure 2) capable of operating in either dry air at warm temperatures or nitrogen from warm to cryogenic temperatures. Elevated pressures in combination with cryogenic temperatures enable testing to the highest Reynolds numbers. The test section is 8.2 by 8.2 by 25 ft. and has a slotted floor and ceiling. In addition, four damping screens in the settling chamber and a contraction ratio of 14.95-to-1 reduce turbulence from the settling chamber to the nozzle throat. Fan-noise effects are minimized by acoustic treatment both upstream and downstream of the fan. Thermal insulation resides inside the pressure shell to aid in maintaining tunnel temperature and thus minimize energy consumption.

The NTF has an operating pressure range of approximately 15 to 125 psia, a temperature range of -250 to +120°F, and a Mach number range of 0.2 to 1.2. The maximum Reynolds number per foot is  $146 \times 10^6$  at Mach 1. When the tunnel is operated cryogenically, heat is removed by the evaporation of liquid nitrogen, which is sprayed into the tunnel circuit upstream of the fan. During this operational mode, venting is necessary to maintain a constant total pressure. When air is the test gas, heat is removed from the system by a water-cooled heat exchanger at the upstream end of the settling chamber. A mixed mode of operation can be used to reach higher Reynolds numbers. This mode uses liquid nitrogen to augment the cooling coil without the expense of fully crossing over into nitrogen mode. Further tunnel details and facility information are provided in Ref. 4.

#### 2. Ames 11-ft Transonic Wind Tunnel

The Ames Unitary Plan Wind Tunnel (UPWT) consists of three tunnel legs: the 11-by-11-Foot Transonic Wind Tunnel (TWT), the 9- by 7-Foot Supersonic Wind Tunnel, and the 8- by 7-Foot Supersonic Wind Tunnel (Figure 3). The two supersonic legs share a common 11-stage axial-flow compressor and aftercooler drive leg, and they use diversion valves at the ends of a common drive leg. A three-stage axial-flow compressor drives the 11-by-11-Foot TWT. A common drive motor system can be coupled to either the 3-stage or 11-stage compressor. One tunnel can therefore be run while test articles are being installed in or removed from the other two.

The 11-by 11-Foot TWT leg, also known as the Ames 11-ft wind tunnel, is a closed circuit, variable-pressure, continuous operation wind tunnel (Figure 4). Subsonic Mach number control involves setting the compressor drive speed to one of ten set points and using variable-camber inlet guide vanes for fine Mach number control. Supersonic Mach number control involves setting the flexible wall nozzle to achieve the proper area ratio in addition to setting the compressor drive speed and the inlet guide vanes. A tandem diffuser system with an annular diffuser followed by a wide-angle diffuser is upstream of a 70-ft-diameter aftercooler section in the drive leg. Flow-smoothing vanes are located in the tandem diffuser to improve flow uniformity entering the heat exchanger and temperature uniformity in the test section. The settling chamber upstream of the contraction is 38 feet in diameter. A Turbulence Reduction System (TRS) located in the settling chamber includes a 1-in.-cell-diameter, 20-in. long honeycomb for flow straightening followed by two 0.041-in.-diameter-wire, 6-mesh screens for turbulence reduction. The contraction provides a transition from the circular cross section of the settling chamber to the square cross section of the test section. The contraction ratio is 9.4. The test section is 11-by 11-feet in cross section and 22 feet in length. Slots in all four walls run the full length of the test section. The slots contain baffles that provide a 6-percent porosity into the plenum chamber. Ejector flaps on all four walls at the exit of the test section can be set remotely to control the plenum flow bypassed from the test section. Flow exits the test section and enters a transition region back to the circular main diffuser. A Plenum Evacuation System (PES) provides an active method of removing air from the test section plenum by using the Make-Up Air (MUA) compressor system of the auxiliaries facility. References 5 and 6 provide more detailed information about the Ames 11-ft wind tunnel.

#### 3. European Transonic Wind Tunnel

The European Transonic Wind Tunnel (ETW) is similar to the National Transonic Facility, a pressurized cryogenic, closed circuit, continuous-flow, fan-driven wind tunnel. It can be operated in closed and slotted wall configurations for testing full and half-models from Mach numbers of 0.15 up to light supersonic conditions at  $M_\infty=1.35$ . Pure high quality nitrogen is used as test gas only. The capability of varying the gas temperature, pressure

and speed independently allows for pure Reynolds number and/or aeroelastic investigations. The test section dimensions are 7.87 ft (2.4 m) in width, 6.56 ft (2 m) in height and about 30 ft (9 m) in length. High flow quality is provided by 2 filling screens in the wide angle diffuser combined with a flow straightener (honeycomb) and 2 anti-turbulence screens followed by a fixed contraction and a flexible nozzle for supersonic operation as given in Figure 5. Additionally, the tunnel features a second throat downstream of the re-entry preventing flow disturbances eventually generated in the high-speed diffuser from propagating upstream into the test-section.

The ETW operating range covers pressures from 110kPa to 450kPa and temperatures from 313K down to 110K allowing the achievement of maximum Reynolds numbers of 50 million for full models and 90 million for semi-span models at a Mach number around 0.85. While the tunnel shell is internally insulated against heat losses the heat generated by the fan is compensated by the evaporation of the injected liquid nitrogen, which is sprayed into the tunnel upstream of the compressor. Further details about the facility and its operation can be found at [www.etw.de](http://www.etw.de).

## B. Model Description

The model used in the current investigation was the NASA Common Research Model. This configuration consists of a contemporary supercritical transonic wing and a fuselage that is representative of a wide-body commercial transport aircraft. The CRM is designed for a cruise Mach number of  $M_\infty = 0.85$  and a corresponding design lift coefficient of  $C_L = 0.5$ . A sketch of the CRM with reference quantities listed is shown in Figure 6. The aspect ratio is 9.0, the leading edge sweep angle is 35 degrees, the wing reference area ( $S$ ) is 3.01 ft<sup>2</sup>, the wing span ( $b$ ) is 62.47 inches, and the mean aerodynamic chord ( $c$ ) is 7.45 inches. The model moment reference center is located 35.8 inches back from the fuselage nose and 2.04 inches below the fuselage centerline. Pressure distributions are measured on both the left and right wings using 291 pressure orifices located in 9 span-wise wing stations ( $\eta = 0.131, 0.201, 0.283, 0.397, 0.502, 0.603, 0.727, 0.846, \text{ and } 0.950$ ). All pressure measurements were made using Electronically Scanned Pressure (ESP) modules mounted inside the forward portion of the fuselage. Based on quoted accuracies from the ESP module manufacturer, surface pressure measurements should be in error no more than  $\pm 0.015$  psi. This in turn would correspond to a variation of no more than  $\pm 0.0026$  in terms of  $C_p$ . The model is mounted in the wind tunnel using a blade sting arrangement in all three tunnels. The only difference between the NTF and Ames 11-ft arrangement occur downstream of the model support system, as shown in Figure 7 and Figure 8. The difference between the sting arrangement of the NTF and ETW begins earlier, i.e., downstream of the blade part of the model support system, as shown in Figure 9. No corrections have been made in any of the data sets for this mounting arrangement. Further details on this geometry are given in Ref. 7.

## C. Test Conditions

### 1. National Transonic Facility

The investigation, conducted over a 6-week period, provided force and moment, surface pressure, model deformation, and surface flow visualization data. Testing was conducted at 5, 19.8 and 30 million Reynolds number. The 5 and 19.8 million Reynolds number data were collected to provide a comparison to previously calculated CFD results and all of the Reynolds numbers were used to provide an assessment of Reynolds number effects. The 19.8 million Reynolds number data were collected at two different  $q_\infty$  levels – a high and a low  $q_\infty$  condition. Having two  $q_\infty$  levels at the same Reynolds number provides an aeroelastic step in the data. All Reynolds number values presented in this paper are based on mean aerodynamic chord. The data were collected at temperatures ranging from -250°F up to 120°F.

All data presented in this paper were obtained at freestream Mach numbers of 0.7 and 0.85. Data were generally obtained over an angle-of-attack range from  $-3^\circ$  to  $+12^\circ$  at 5 million Reynolds number and from  $-3^\circ$  to  $+6^\circ$  at 19.8 and 30 million Reynolds numbers. The reduced angle-of-attack range at the higher Reynolds number was required such that safe model stress levels would not be exceeded. Flow angularity measurements were made and upflow corrections ranging from  $0.092^\circ$  to  $0.173^\circ$  were applied to the final NTF data. Classical wall corrections accounting for model blockage, wake blockage, tunnel buoyancy, and lift interference have been applied.

In order to ensure a consistent and repeatable transition from laminar to turbulent flow and to support the goal of the wind tunnel data being used for CFD validation purposes, it was important to apply a proven and reliable method to fix transition on the model. Evercoat trip dots measuring 0.05 inches in diameter and spaced 0.1 inches apart (center to center) were used for the current investigation. For a chord Reynolds number of 5 million, a trip dot height of 0.0035 inches was used from the SOB (side of body) to the yehudi break and 0.003 inches was used from the yehudi break to the wing tip. These trip dots were installed at 10% chord. Vinyl adhesive trip dots were applied at the nose of the fuselage and left on for the entire test. When the tails were on the model, trip dots were located at 10% chord and measured 0.003 inches.

Another important set of data obtained in this investigation was model deformation measurements. Since an effective correlation of computational and experimental data will be directly tied to how well the computational and experimental model geometries match one another, it is important to obtain an accurate definition of the model geometry as tested under aerodynamic loads. In order to obtain this information, a video model deformation measurement technique<sup>8</sup> has been developed and employed multiple times at the NTF. This system was used in the current investigation to obtain wing deflection and twist measurements due to aerodynamic loading and this data is presented herein.

## 2. Ames 11-ft Wind Tunnel

The investigation, conducted over a 5-week period, provided force and moment, surface pressure, and surface flow visualization data. Testing was conducted at a chord Reynolds number of 5 million. The data were collected at temperatures of approximately 100° F.

All data presented in this paper were obtained at freestream Mach numbers of 0.7 to 0.85. Data were generally obtained over an angle-of-attack range from -3° to +12° at 5 million chord Reynolds number. Flow angularity measurements were made and upflow corrections ranging from 0.013° to 0.067° were applied to the final data. Classical wall corrections accounting for tunnel buoyancy and lift interference have been applied.

Transition was also fixed on the model when tested at the Ames 11-ft wind tunnel. For this investigation, though, only vinyl adhesive trip dots were applied. These trip dots measured 0.05 inches in diameter and were spaced 0.1 inches apart. For a chord Reynolds number of 5 million, a trip dot height of 0.0035 inches was used from the SOB (side of body) to the yehudi break, and 0.003 inches was used from the yehudi break to the wing tip. These trip dots were installed at 10% chord. Vinyl adhesive trip dots were also applied at the nose of the fuselage and left on for the entire test. Finally, when the tails were on the model, trip dots were located at 10% chord and measured 0.003 inches.

## 3. European Transonic Wind Tunnel

Since this investigation was funded by the European Commission as part of the ESWIRP project, the available budget only allowed for testing over a limited range of conditions. The test plan for the 5-day test campaign in the ETW was determined based on a compromise between test requirements from the European project group chaired by J.L. Goddard from ONERA-France which focused on acquiring data for CFD validations of unsteady wake flows and a repeat of the conditions at which the used CRM model had been tested in the NTF. A few polars were added at a very low Reynolds number to provide comparative aerodynamic data for the Japanese research organisation JAXA who have tested the CRM in a downscaled version in their transonic tunnel.

For achieving the scientific goal of the project, newly integrated measurement capabilities were operated during the campaign: unsteady PIV for wake flow analysis and unsteady and steady model deformation measurements combined with the recording of unsteady balance signals taking the benefit of an upgraded fast high capacity data acquisition system. In the frame of the present paper only aerodynamic data like force, moments and wing pressure distributions combined with the wing deformation are presented. Although, data were acquired at 12 different Mach numbers ranging from 0.25 to 0.87 the majority focussed on  $M=0.7$  and the model design Mach number of 0.85. So, with respect to the intended comparison of results, the reference test conditions of the NTF at these two Mach numbers were carefully set and controlled. To cover the relevant Reynolds numbers of 5, 19.8 and 30 million the tunnel temperature was varied between 302 K and 117 K combined with corresponding pressures between 200 and 300 kPa. As to be seen in Figure 10, the operating envelopes of NTF and ETW do not allow achieving the minimum and maximum Reynolds number at the identical  $q/E$  value. Hence, it was decided to duplicate the 19.8 million Reynolds number at a lower and higher  $q/E$  value allowing an additional comparison of the model deformation assessment as a function of the different aeroelastic effects. By performing lift polars with the model in upright and inverted position the upwash could be assessed as 0.010 to 0.015 deg over the full operating range. The measured data were additionally corrected for wall interference based on the ETW experimental assessment established in the past. Extreme care is always given to the measurement of the model angle of attack. Before starting the test campaign the electrical offset and misalignment of the relevant inclinometer inside the model is checked even under load applied to it. Special care was also given to the application of the transition band classically used when testing at a chord Reynolds number of 5 million. Performing this work in close cooperation with the NTF experts minimised the risk for later mismatches in the results originated by this sensitive item.

Before facilities like NTF and ETW went into operation engineers were convinced of the rigidity of wind tunnel models not suffering remarkable deformations generated by aerodynamic loads especially present in pressurised facilities. Using the unique capabilities of these tunnels for establishing identical Reynolds numbers at different pressure or better  $q/E$  levels the opposite could be proven. Nowadays, the correct assessment of the wing shape under load is mandatory for all comparisons to CFD results. Starting with the developments of appropriate

measurement systems with a Moirée tool today, ETW may operate 4 systems in parallel, e.g. for monitoring the shape of the main wing and all high lift components of a half-model. The Stereo Pattern Tracking systems (SPT) are capable of monitoring the shift in space of markers pasted on the lower wing surface as to be seen in Figure 9. In the test campaign reported here one system was looking on the main wing with 58 frames/sec while a second one monitored unsteady HTP movements with 386 frames/sec. More details and results can be found in Reference 9.

### III. Results and Discussion

#### A. Force & Moment Comparisons

One of the primary purposes of this paper is to present the comparison data between the NASA tunnels and the ETW wind tunnel. First, the lift, drag and pitching moment are examined. Figures 11 and 12 show the comparisons between all three wind tunnels at  $Re_c=5 \times 10^6$ . These figures show that at this Reynolds number, the NTF drag data is  $\sim 1$  count higher than the ETW data and is 5 counts higher than the Ames data for the  $M=0.7$  case and the NTF drag data is 16 counts lower than the ETW data and 5 counts higher than the Ames data for the  $M=0.85$  case. The NTF lift data is lower than both the Ames and ETW data and the pitching moment is more nose down than the Ames data but less nose down than the ETW data for both Mach numbers presented.

Figures 13 and 14 show the lift, drag and pitching moment comparisons for the  $Re_c=19.8 \times 10^6$  case at a low  $q_\infty$  value. At Mach = 0.7, the drag data is almost identical, the NTF lift data is lower than the ETW data and the pitching moment is less nose down than the ETW data. For the Mach=0.85 case, the NTF drag data is 12 counts lower than the ETW data, the NTF lift data is lower than ETW and the pitching moment is once again predicting less nose down than ETW.

The results for the  $Re_c=19.8 \times 10^6$  case at a high  $q_\infty$  value cases are given in Figures 15 and 16. For Mach=0.7, the drag data is again almost identical between the two tunnels, the NTF lift data is lower than the ETW data and the NTF pitching moment data is once again predicting a less nose down value than the ETW data. At Mach = 0.85, a similar picture is seen. At this Mach number, the NTF drag data is 10 counts lower than the ETW data and the NTF lift data is lower than the ETW lift data and the pitching moment is once again predicting less nose down moment than the ETW data.

At a flight Reynolds number of  $Re_c=30 \times 10^6$ , the comparisons show essentially the same differences as for the  $Re_c=19.8 \times 10^6$  at a high  $q_\infty$  case, as shown in Figures 17 and 18. For Mach=0.7, the NTF and ETW drag data are almost identical, the NTF lift data is lower than the ETW data and the NTF pitching moment data is less nose down than ETW. At Mach=0.85, the NTF drag data is 9 counts lower than the ETW data, the NTF data is lower than ETW and the pitching moment data is less nose down than ETW.

#### B. Surface Pressure Comparisons

Another goal of these investigations was to examine the surface pressure differences between the NTF and ETW wind tunnels. Figures 19 through 26 show the surface pressure distributions for the Mach=0.7 and 0.85 cases at  $Re_c=5, 19.8$  and  $30$  million. In each of these figures, two points are given for the ETW data. These two points were chosen such that they bracket the  $C_L$  value of the NTF data. This does result in comparison of different angles of attack but closer comparison of the  $C_L$  values. For most of the Mach and Reynolds numbers plotted, the data compares very well across the entire wing. There are several minor differences between the data sets but only a few major differences are seen. The first major difference is seen in Figure 20. At Mach=0.85,  $Re_c=5 \times 10^6$ , the shock on the wing at  $\eta=0.603$  is stronger in the ETW data than in the NTF data. The only other major difference is shown on Figure 26, which is the Mach=0.85,  $Re_c=30 \times 10^6$  comparison. At this condition, the shock on the wing at  $\eta=0.502$  is stronger in the NTF data than in the ETW data.

#### C. Wing Bending & Twist Comparisons

The wing bending and twist was measured in both the NTF and the ETW during testing of the CRM. The comparison of the results of these measurements are shown in Figures 27 through 32 for Mach numbers of 0.7 and 0.85 and Reynolds numbers ranging from 5 to 30 million. There was no data taken at Mach=0.7 at  $Re_c=5$  or 30 million therefore no comparisons are given herein for these conditions. The data that is shown indicates that the wing twist and wing bending at the two wind tunnels agree well, mostly within the accuracy of the data taken.

## IV. Summary

A successful investigation of the new NASA Common Research Model has been completed in the National Transonic Facility, the Ames 11-ft Wind Tunnel and the European Transonic Wind Tunnel. Data have been obtained at chord Reynolds numbers of 5 million for the WBT0 configuration in all three wind tunnels and in addition, at Reynolds numbers of 19.8 and 30 million in the NTF and ETW. Force and moment, surface pressure, wing bending and twist data are presented herein. Tunnel-to-tunnel effects have been assessed for all of these data.

- 1) For all of the data presented herein, the NTF data predicted a lower lift value than both the Ames 11-ft and ETW.
- 2) The drag differences varied depending on Mach and Reynolds number. At a  $M=0.7$  and  $Rec=5 \times 10^6$ , the NTF drag data was higher than the ETW and Ames 11-ft data but at  $M=0.7$  at the other three Reynolds number and dynamic pressure conditions, the NTF and ETW drag data were almost identical. For all of the  $M=0.85$  cases presented, the NTF drag data is predicted lower than the ETW data by as much as 16 drag counts.
- 3) At a Reynolds number of 5 million based on chord, the NTF pitching moment was more nose down than the Ames 11-ft data but less nose down than the ETW data. At the other three Reynolds number and dynamic pressure conditions, the NTF data was consistently predicted as being less nose down than the ETW data.
- 4) All of the surface pressures presented herein show good agreement between the NTF and ETW data across the wing, with only a couple of exceptions.
- 5) The wing bending and twist data agree well – to within data tolerance for most of the conditions presented herein.

## Acknowledgments

The authors would like to gratefully acknowledge the efforts of the NASA and ETW teams throughout all phases of these experimental investigations. NTF, Ames 11-ft and ETW staff are recognized for their efforts in effectively obtaining all desired experimental data.

## References

- <sup>1</sup> Lutz, Thorsten, Gansel, Philipp, Godard, Jean-Luc, Gorbushin, Anton, Konrath, Robert, Quest, Jürgen, and Rivers, S. Melissa B., “Going for Experimental and Numerical Unsteady Wake Analyses Combined with Wall Interference Assessment Using the NASA CRM Model in ETW,” AIAA Paper 2013-0871, *51<sup>st</sup> AIAA Aerospace Sciences Meeting including the New Horizons Forum and Aerospace Exposition*, Grapevine, TX, January 2013.
- <sup>2</sup> Konrath, Robert, “High-Speed PIV Applied to Wake of NASA CRM Model in ETW Under High Re-Number Stall Conditions for Sub- and Transonic Speeds,” *53<sup>rd</sup> AIAA Aerospace Sciences Meeting*, Kissimmee, FL, January 2015, (submitted for publication).
- <sup>3</sup> Gloss, B. B., “Current Status and Some Future Test Directions for the US National Transonic Facility. Wind Tunnels and Wind Tunnel Test Techniques,” *Royal Aeronautical Society*, 1992, pp. 3.1-3.7.
- <sup>4</sup> Fuller, D. E., “Guide for Users of the National Transonic Facility,” *NASA TM-83124*, 1981.
- <sup>5</sup> Kmak, F., “Modernization and Activation of the NASA Ames 11-by-11-Foot Transonic Wind Tunnel,” AIAA Paper 2000-2680, *21st Aerodynamic Measurement Technology and Ground Testing Conference*, June 2000.
- <sup>6</sup> Amaya, M.A. and Murthy, S.V., “Flow Quality Measurements in the NASA Ames Upgraded 11-by-11-Foot Transonic Wind Tunnel (invited Paper),” AIAA Paper 2000-2681, *21st Aerodynamic Measurement Technology and Ground Testing Conference*. June 2000.
- <sup>7</sup> J. C. Vassberg, M. A. DeHaan, S. M. Rivers, and R. A. Wahls. “Development of a Common Research Model for Applied CFD validation studies.” AIAA Paper 2008-6919, *26th AIAA Applied Aerodynamics Conference*, Hawaii, HI, August 2008.
- <sup>8</sup> Burner, A. W. and Liu, T., “Videogrammetric Model Deformation Measurement Technique,” *Journal of Aircraft*, Vol. 38, No. 4, July-August 2001, pp. 745-754.
- <sup>9</sup> Quix, H., Hensch, A.K., “Dynamic Measurements on the NASA CRM Model tested in ETW,” *53<sup>rd</sup> AIAA Aerospace Sciences Meeting*, Kissimmee, FL, January 2015, (submitted for publication).



Figure 1. Aerial view of the National Transonic Facility.

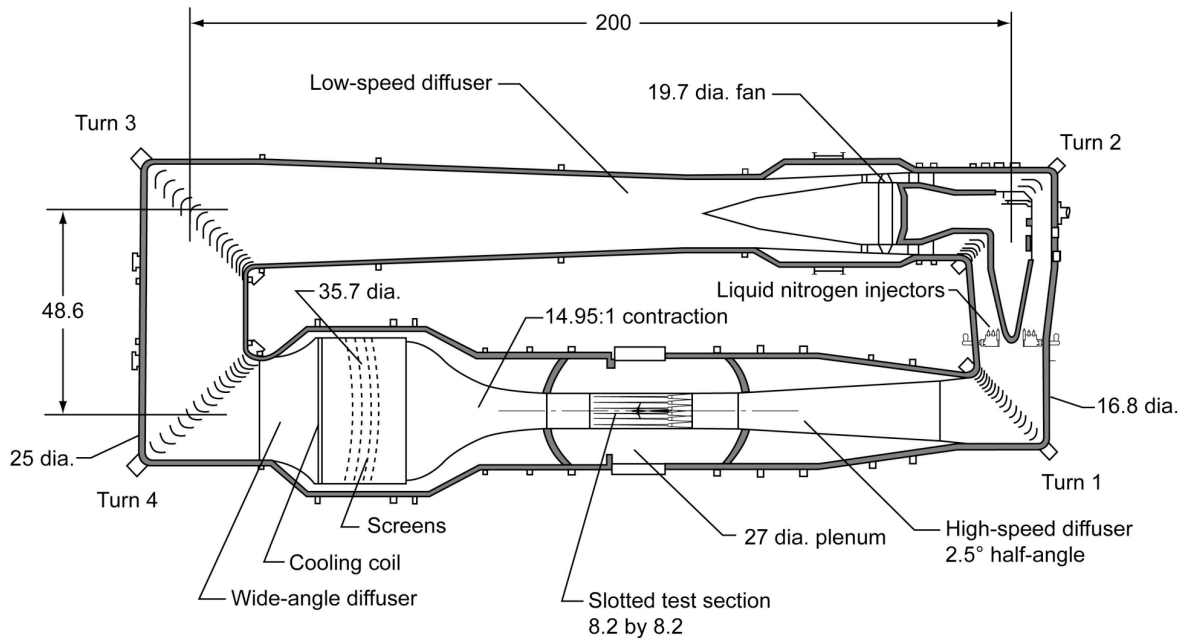
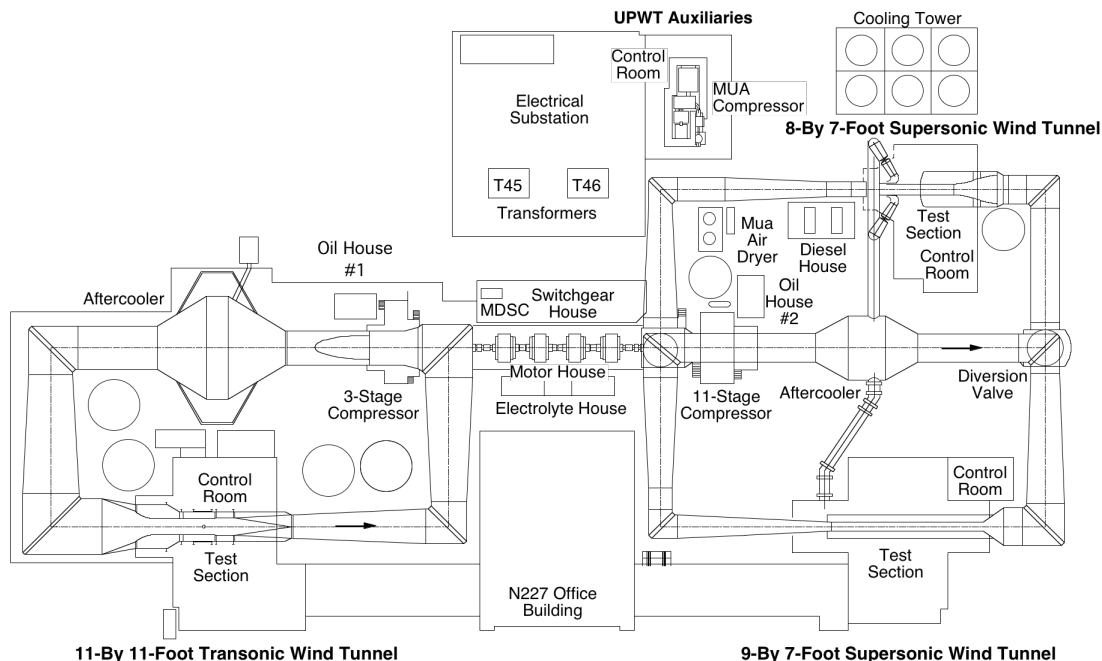
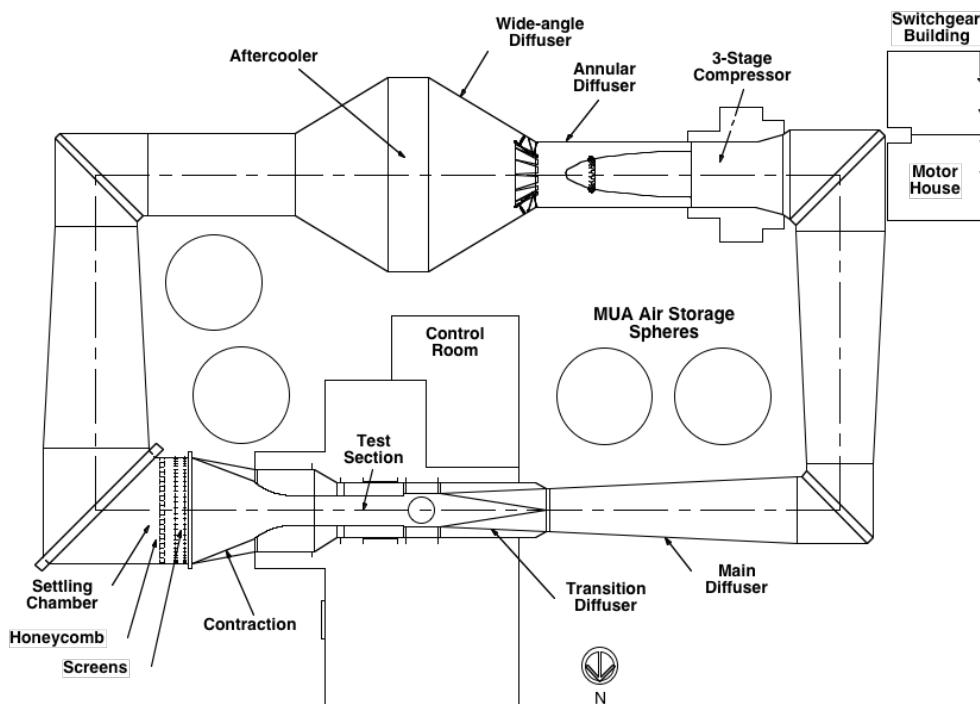


Figure 2. Sketch of the National Transonic Facility tunnel circuit. Linear dimensions are given in feet.



**Figure 3. Unitary Plan Wind Tunnel (UPWT) at the NASA Ames Research Center.**



**Figure 4. Sketch of the Ames 11-Foot Wind Tunnel.**

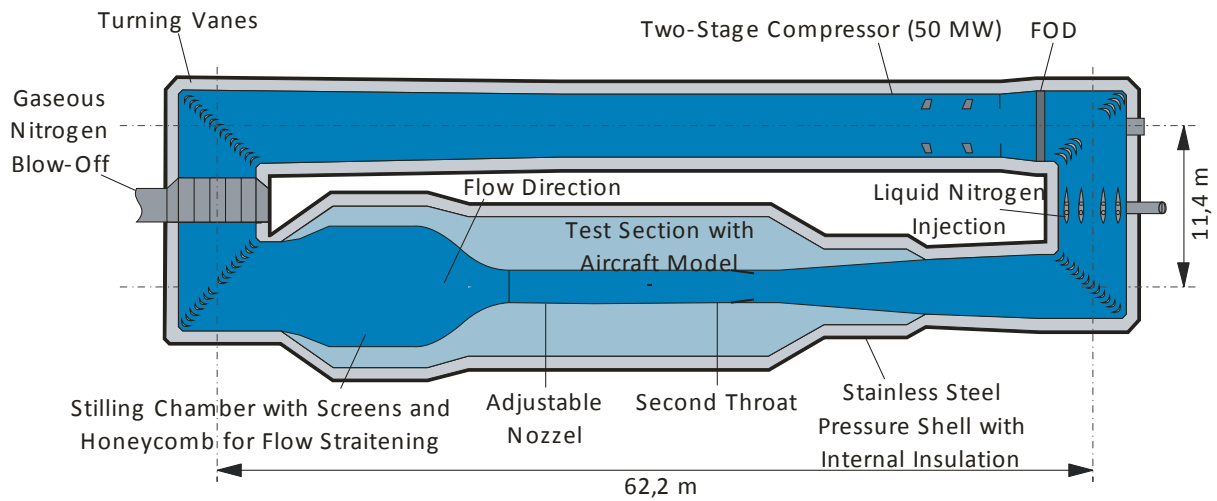
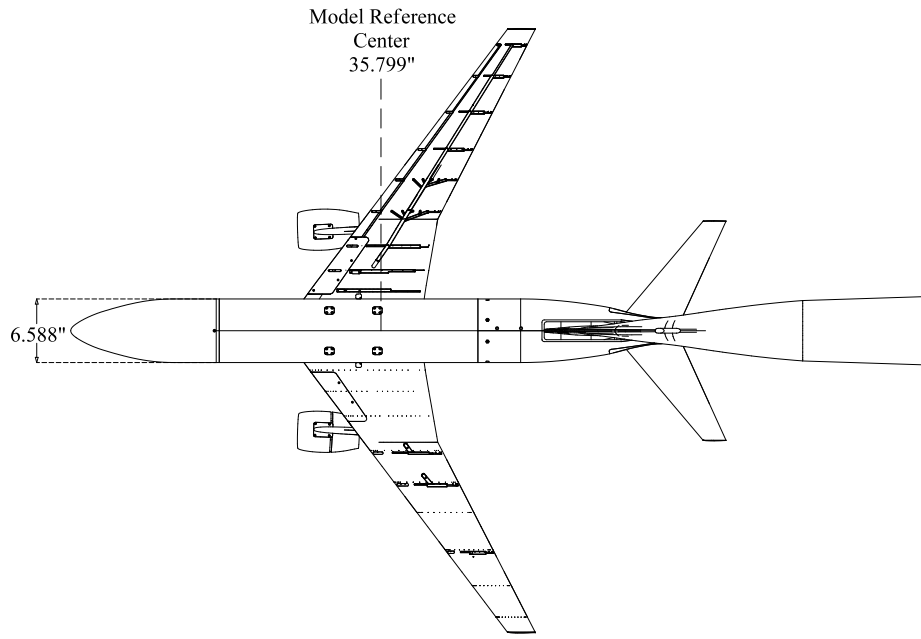
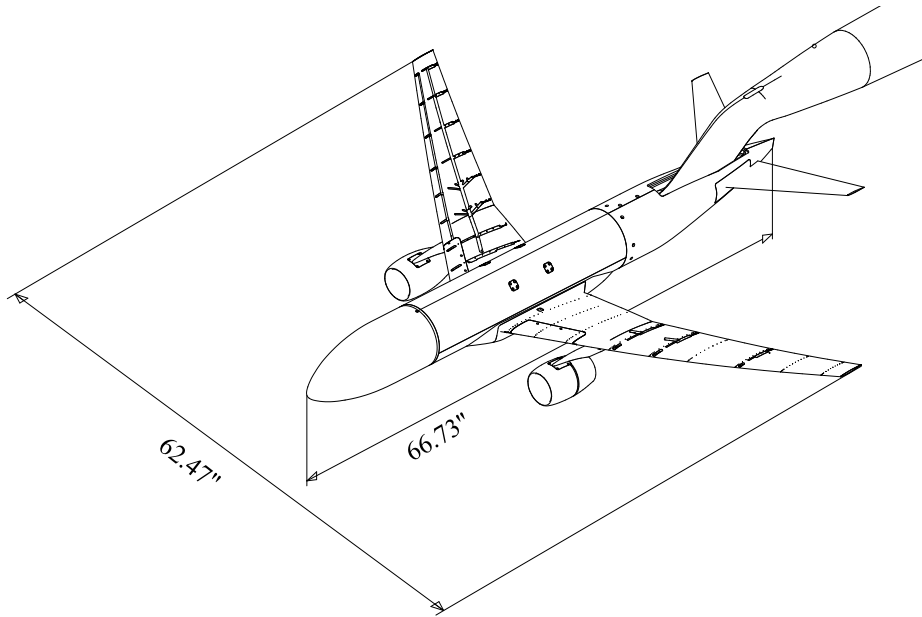


**Figure 5. Sketch of the European Transonic Wind Tunnel aerodynamic circuit.**

Downloaded by NASA LANGLEY RESEARCH CENTRE on January 30, 2018 | http://arc.aiaa.org | DOI: 10.2514/6.2015-1093



a) Top View



b) Isometric View

**Figure 6. Sketch of the Common Research Model with reference quantities.**

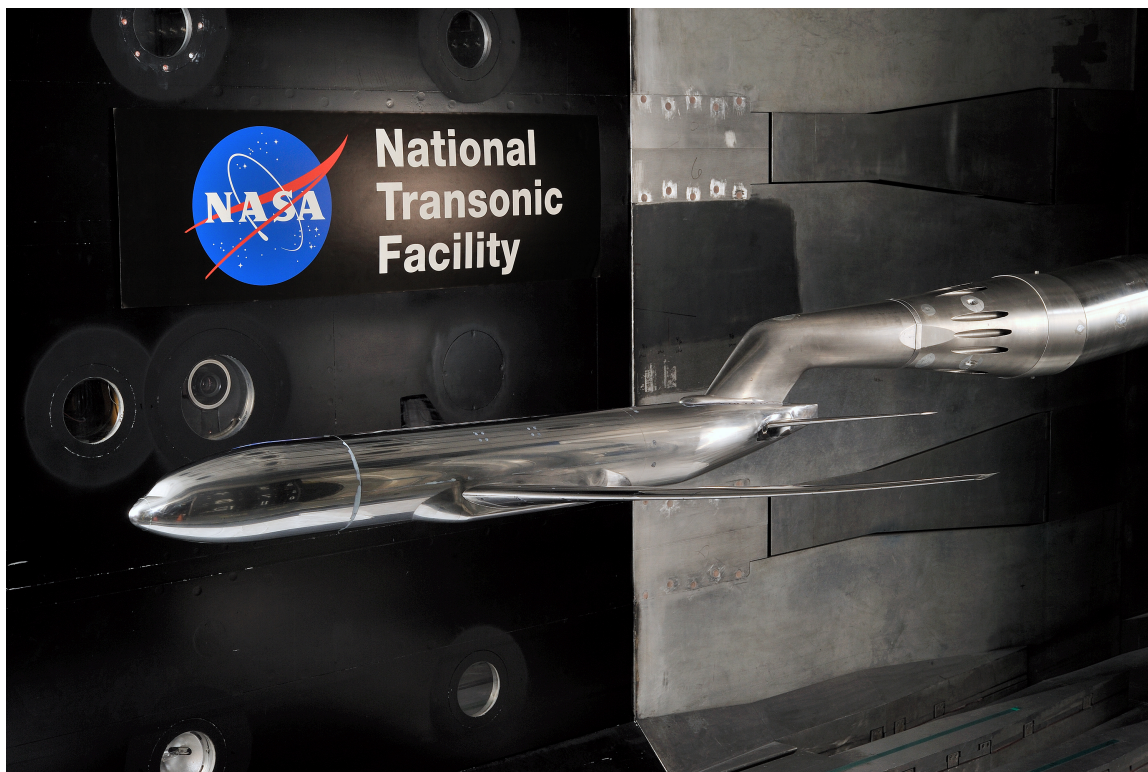


**Figure 7. Photo of the Common Research Model in the National Transonic Facility.**



**Figure 8. Photo of the Common Research Model in the Ames 11-ft Wind Tunnel.**

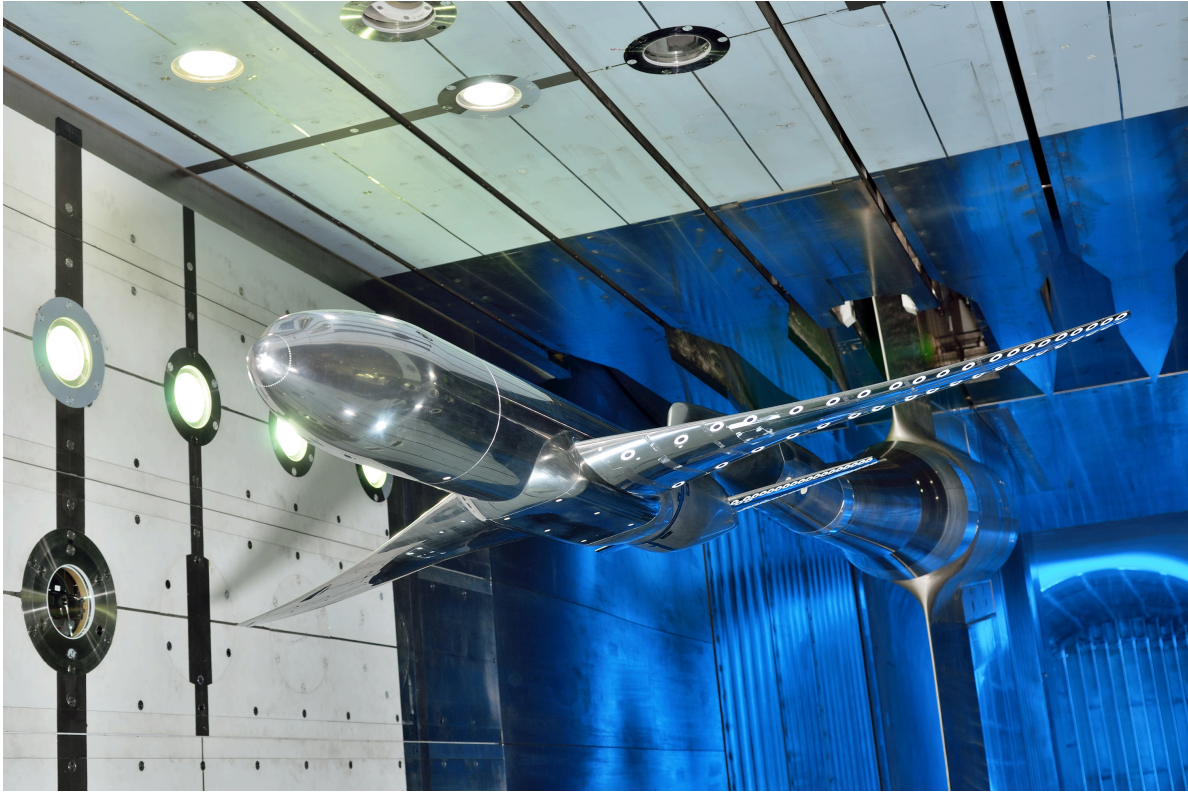


Figure 9. Photo of the Common Research Model in the European Transonic Wind Tunnel.

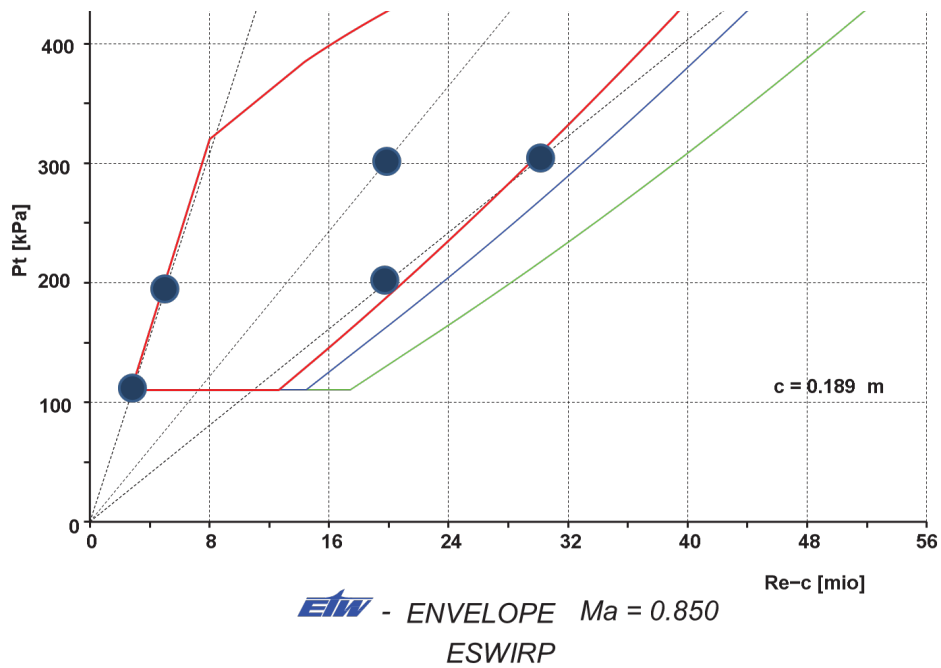
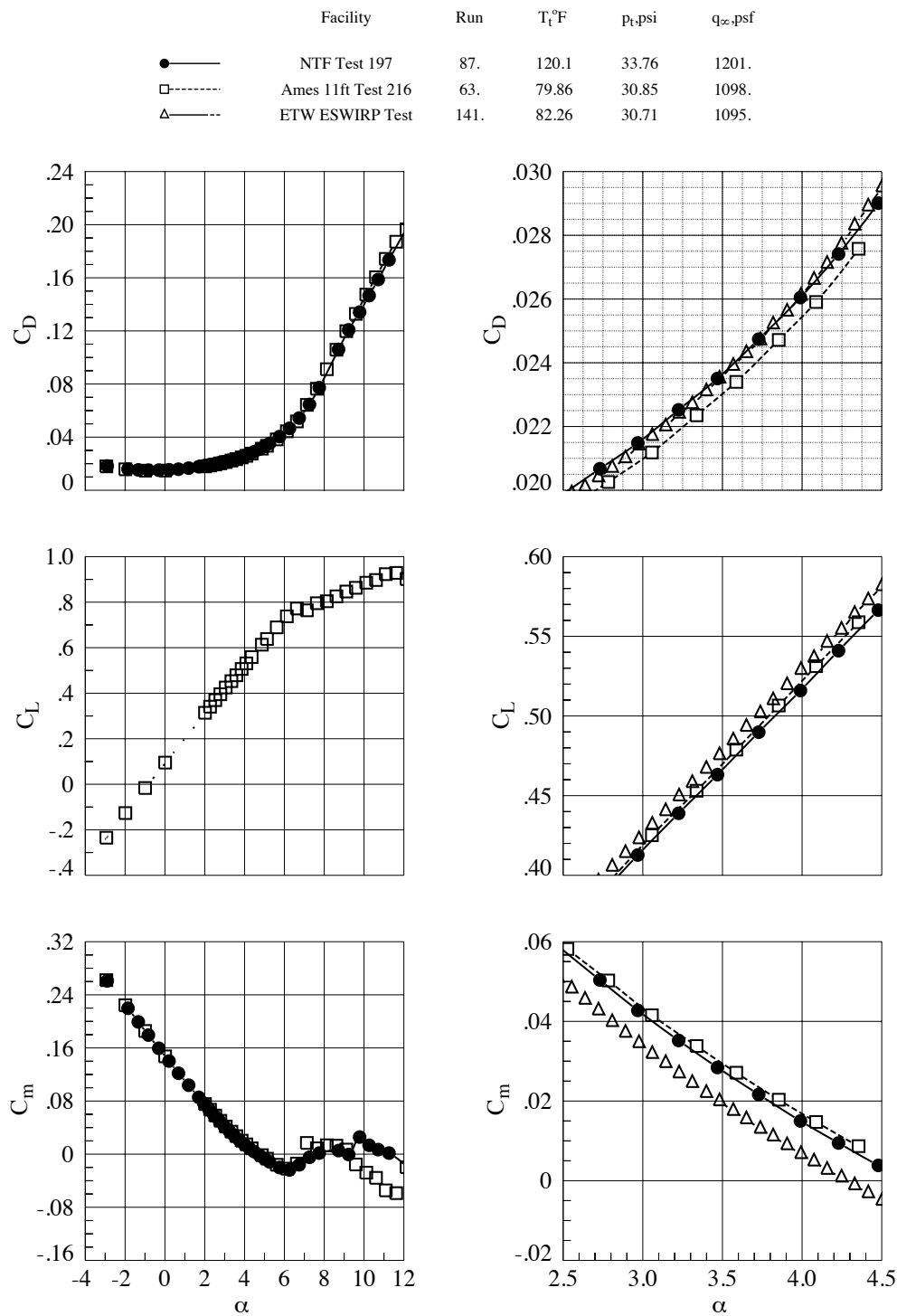
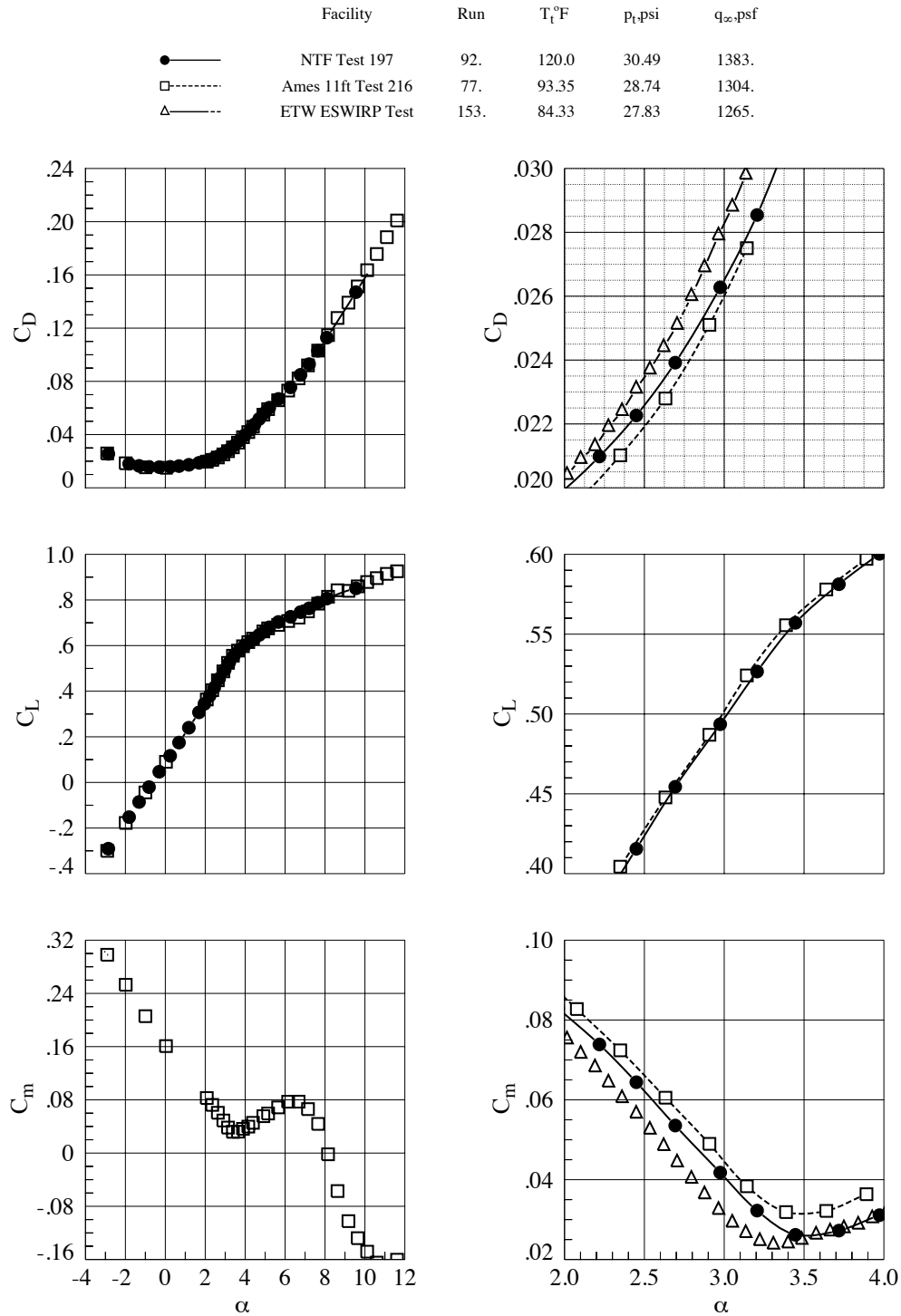


Figure 10. ETW test envelope at Mach = 0.85.



**Figure 11. Lift, drag and pitching moment coefficients, Mach = 0.7,  $Re_c = 5 \times 10^6$ .**



**Figure 12. Lift, drag and pitching moment coefficients, Mach = 0.85,  $Re_c = 5 \times 10^6$ .**

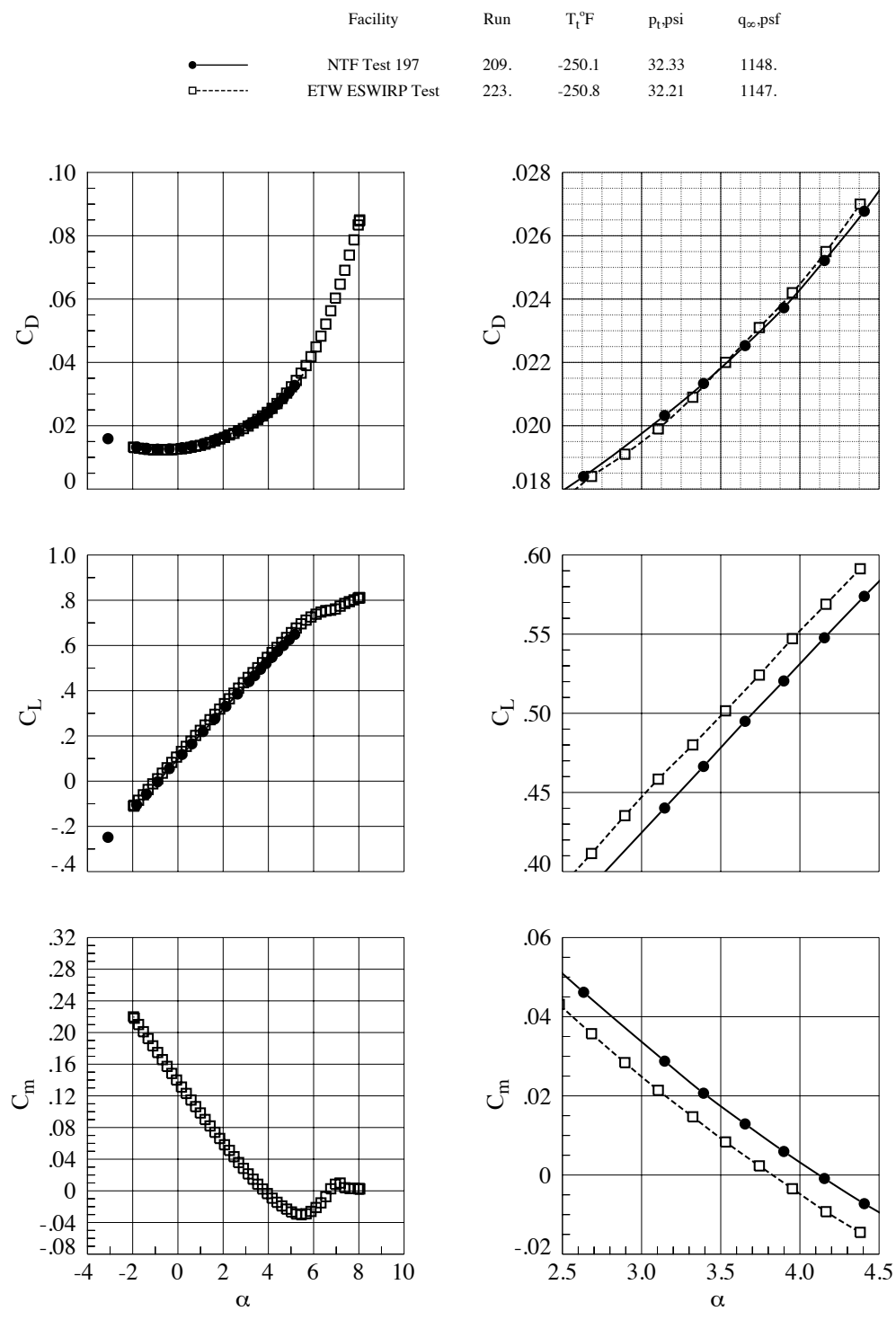
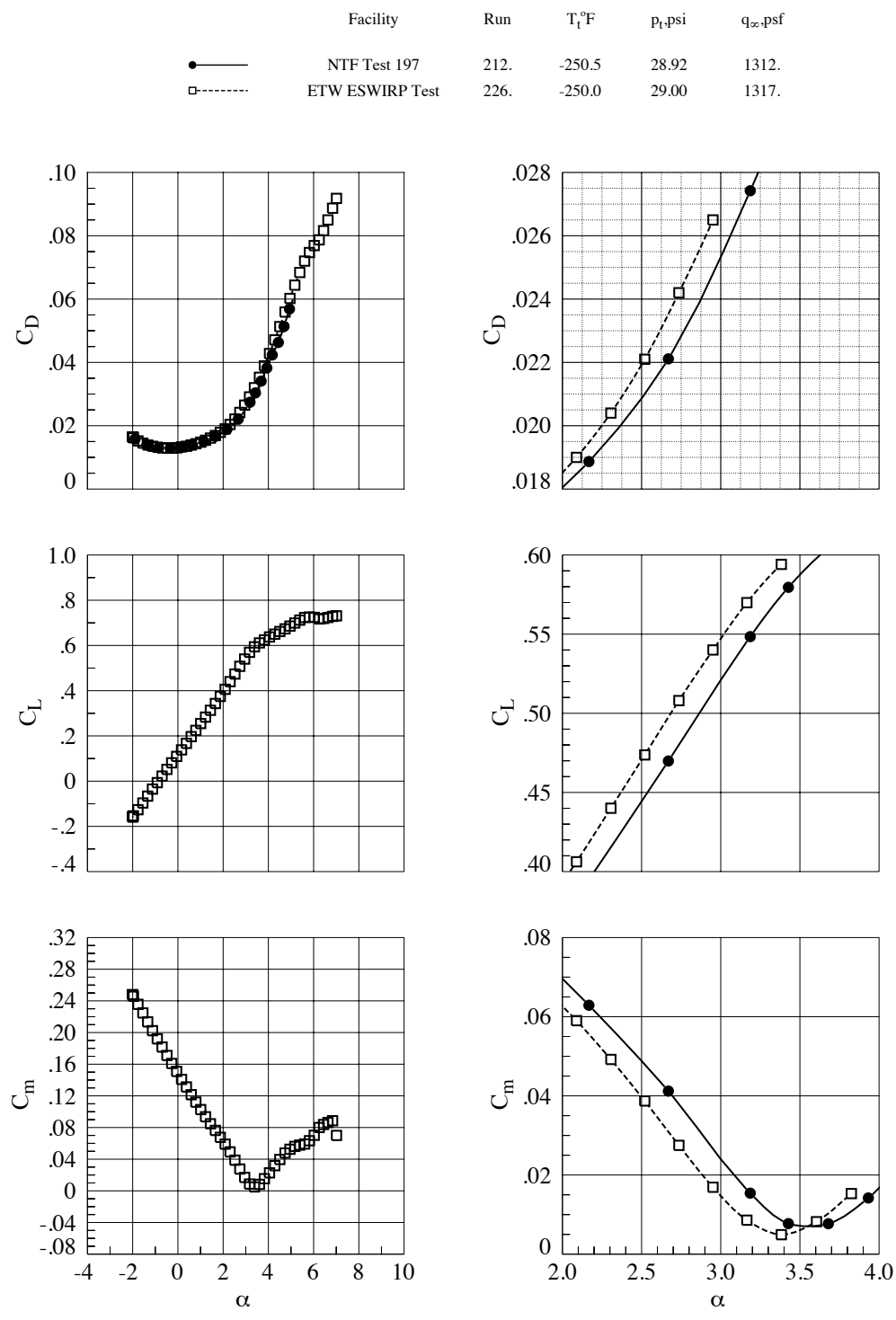
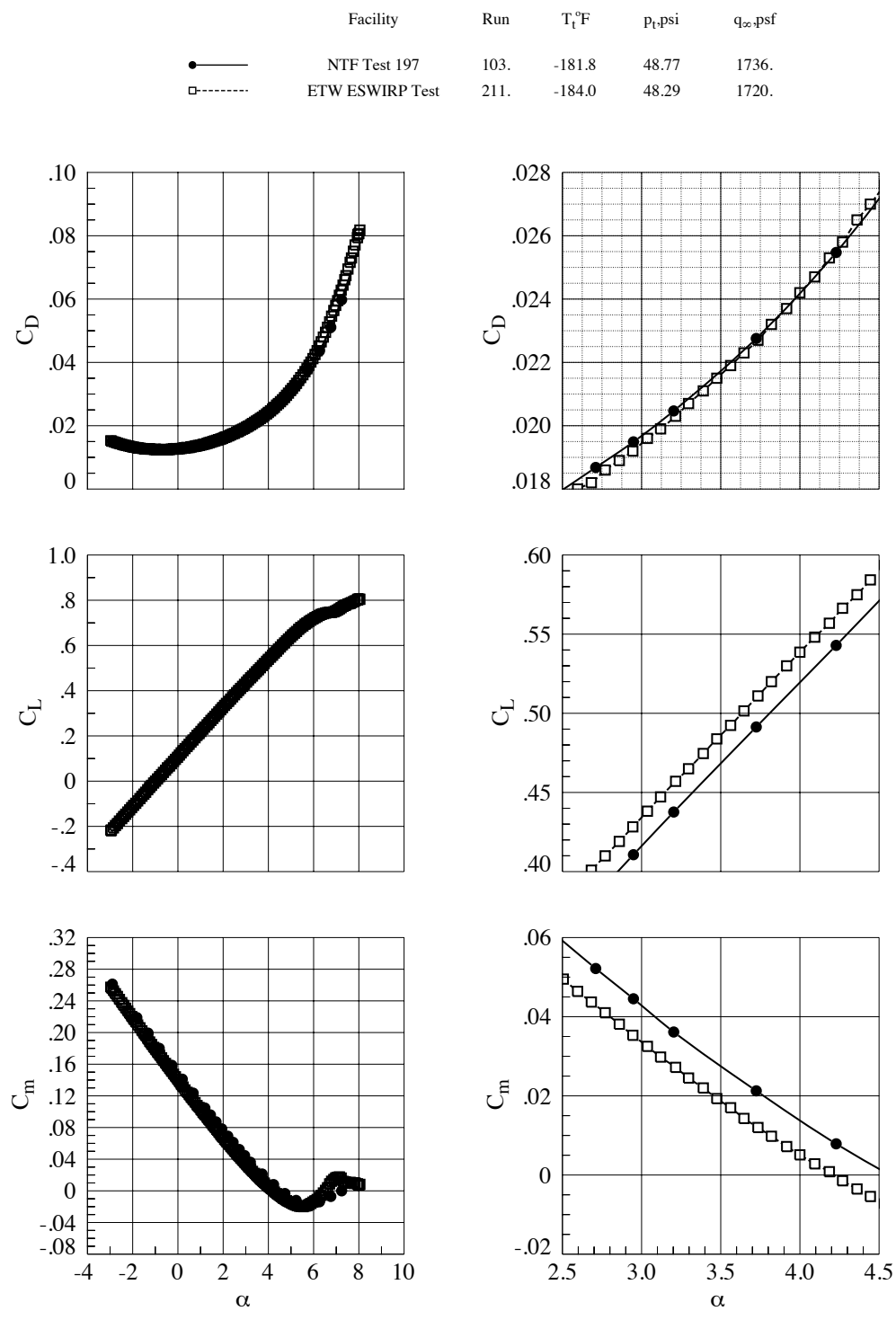


Figure 13. Lift, drag and pitching moment coefficients, Mach = 0.7,  $Re_c = 19.8 \times 10^6$ ,  $q_\infty = 1148$  psf.



**Figure 14. Lift, drag and pitching moment coefficients, Mach = 0.85,  $Re_c = 19.8 \times 10^6$ ,  $q_\infty = 1312$  psf.**



**Figure 15. Lift, drag and pitching moment coefficients, Mach = 0.7,  $Re_c = 19.8 \times 10^6$ ,  $q_\infty = 1736$  psf.**

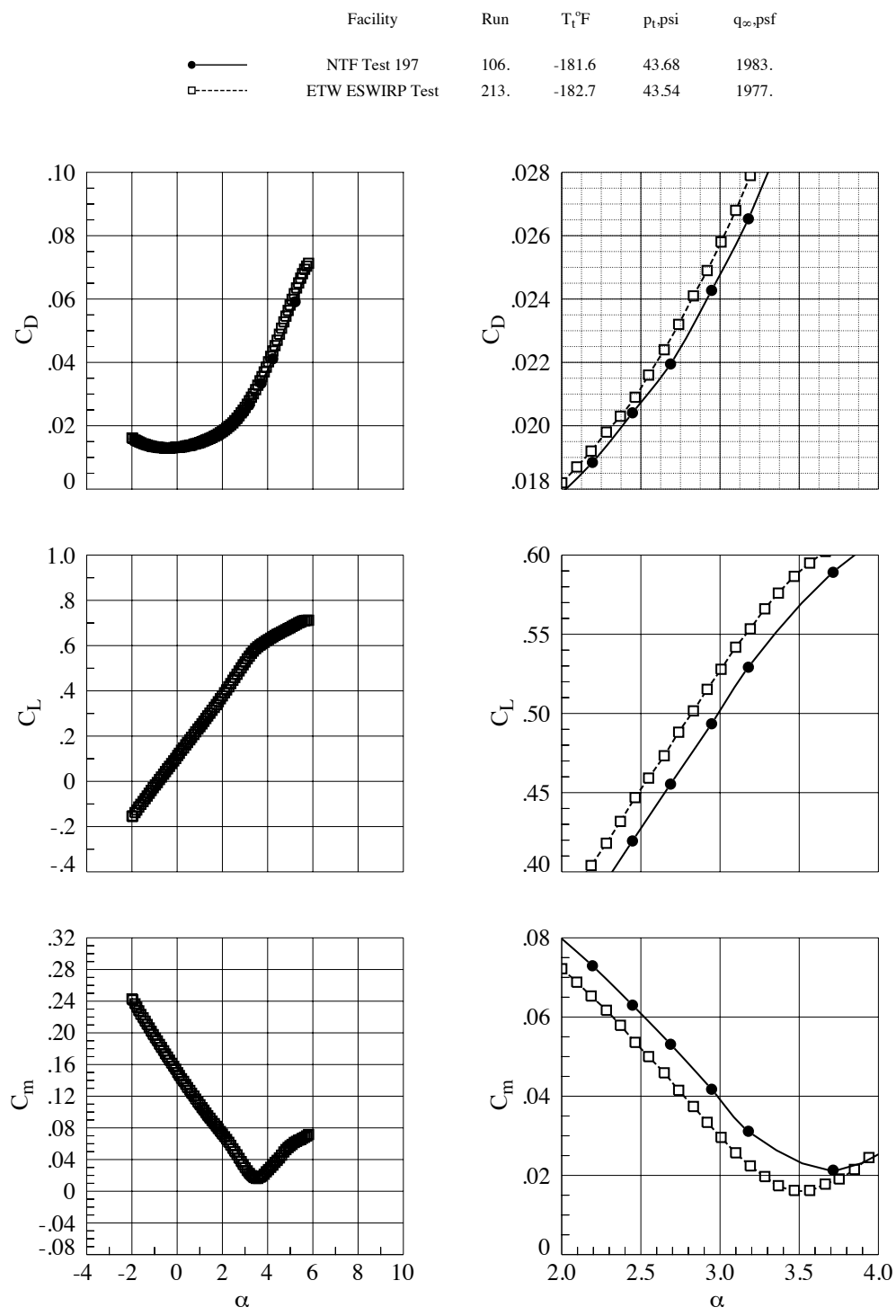


**Figure 16. Lift, drag and pitching moment coefficients, Mach = 0.85,  $Re_c = 19.8 \times 10^6$ ,  $q_\infty = 1983$  psf.**

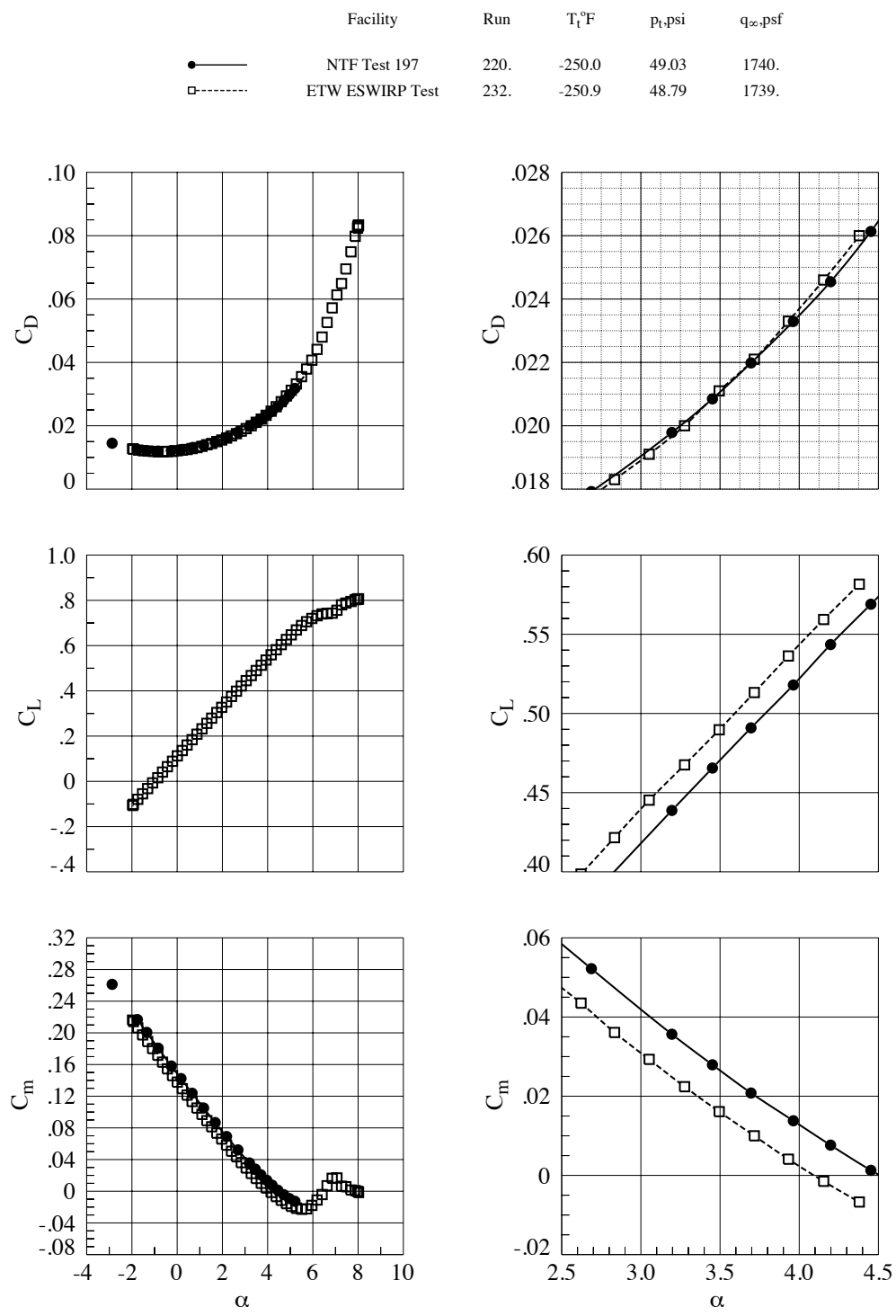


**Figure 17. Lift, drag and pitching moment coefficients, Mach = 0.7, Re<sub>c</sub> = 30x10<sup>6</sup>, q<sub>∞</sub> = 1740 psf.**

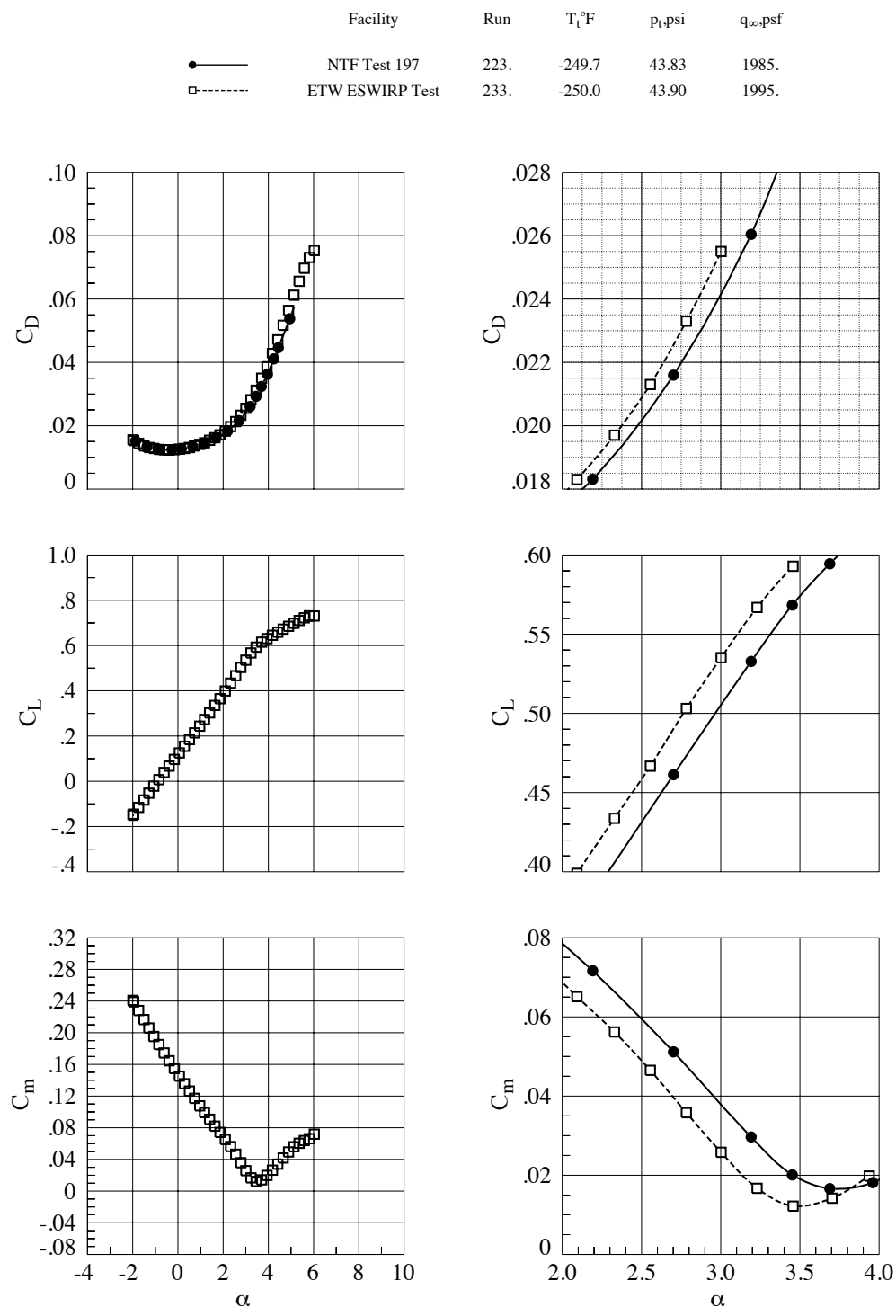


Figure 18. Lift, drag and pitching moment coefficients, Mach = 0.85,  $Re_c = 30 \times 10^6$ ,  $q_\infty = 1985$  psf.

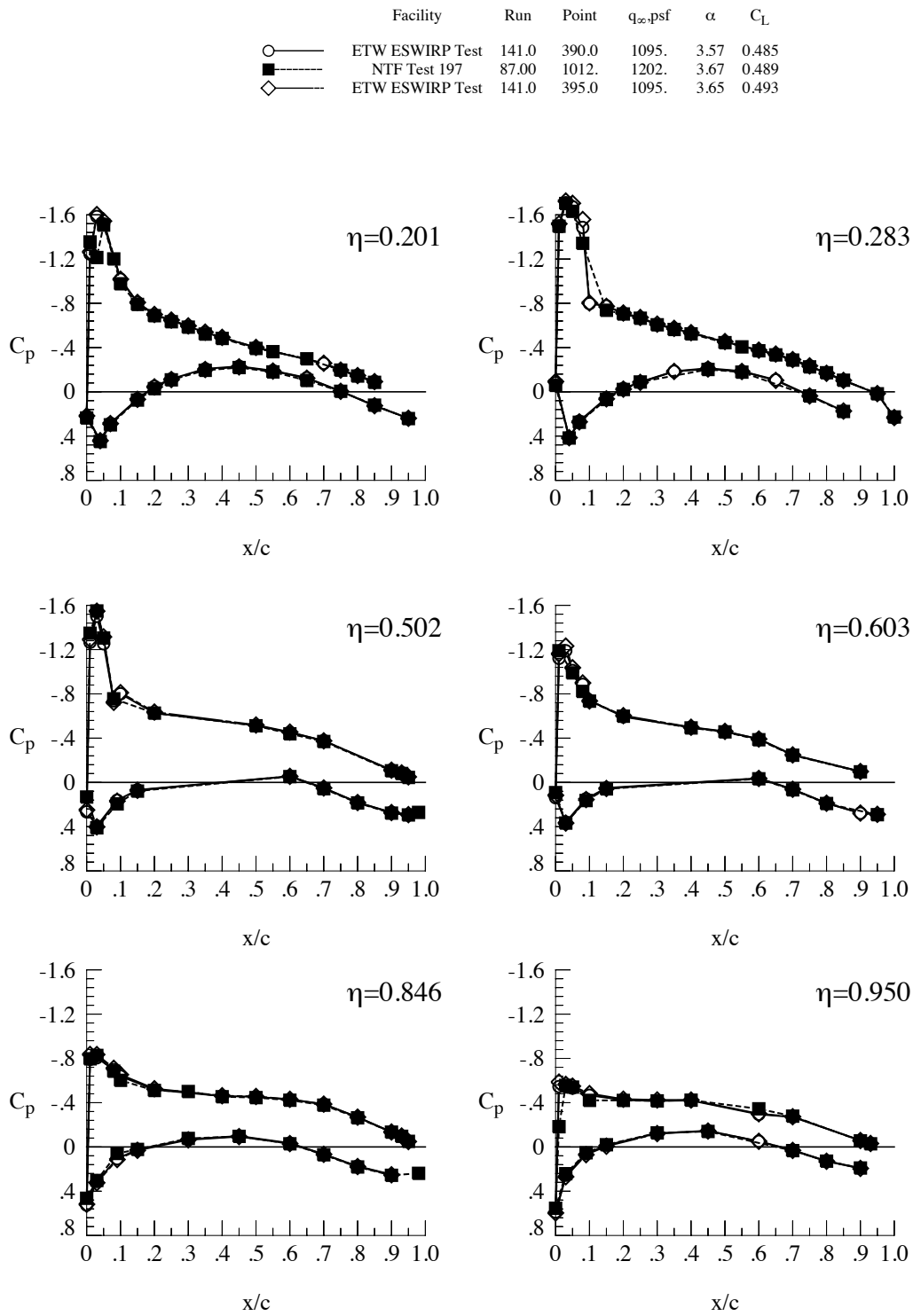


Figure 19. Surface pressures, Mach = 0.7,  $Re_c = 5 \times 10^6$ .

	Facility	Run	Point	$q_{\infty}$ -psf	$\alpha$	$C_L$
○	ETW ESWIRP Test	153.0	340.0	1264.	2.79	0.486
■	NTF Test 197	92.00	1149.	1384.	2.94	0.493
◇	ETW ESWIRP Test	153.0	345.0	1264.	2.88	0.498

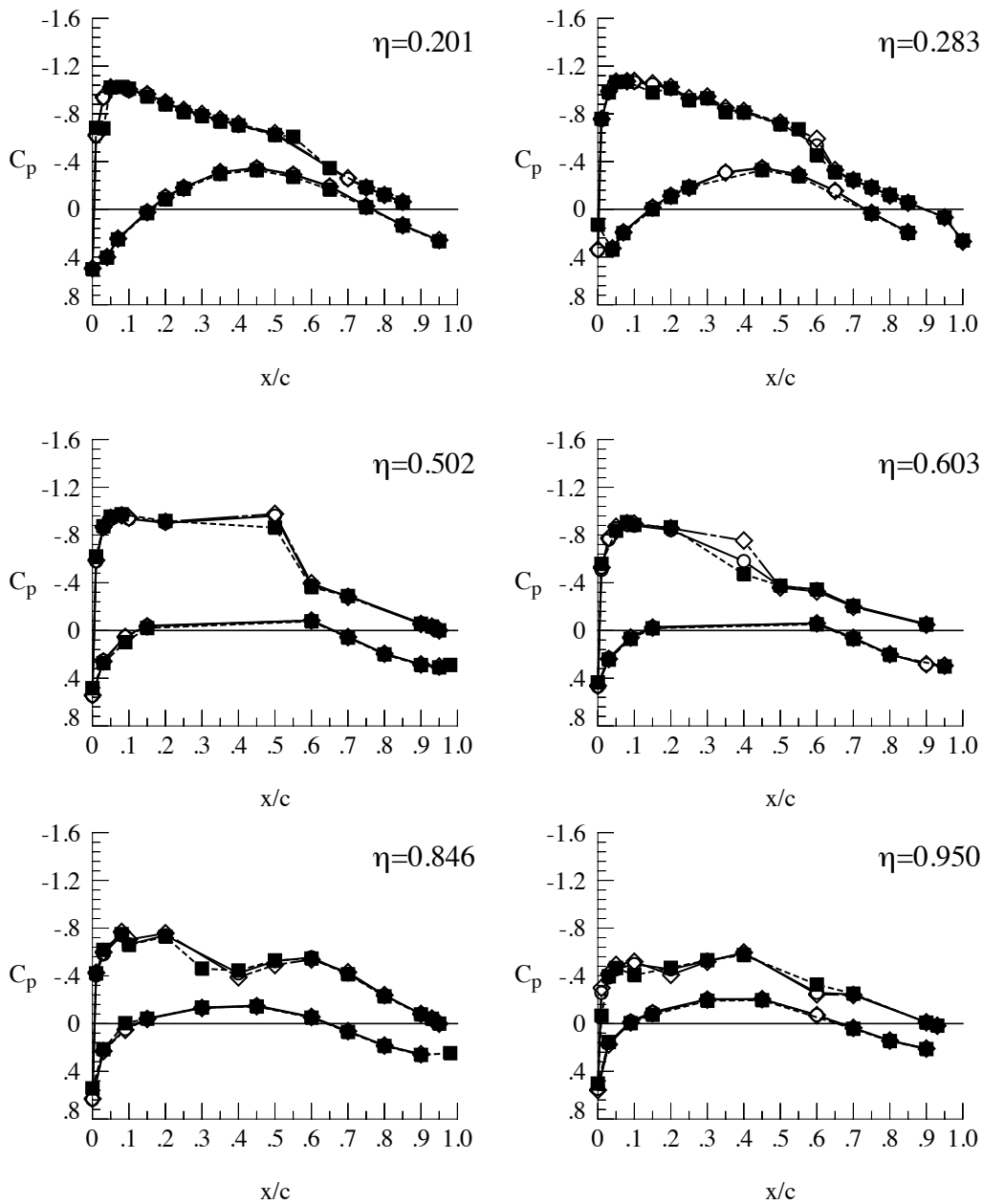


Figure 20. Surface pressures, Mach = 0.85,  $Re_c = 5 \times 10^6$ .

	Facility	Run	Point	$q_\infty$ -psf	$\alpha$	$C_L$
○	ETW ESWIRP Test	223.0	130.0	1147.	3.32	0.480
■	NTF Test 197	209.0	2743.	1148.	3.60	0.495
◇	ETW ESWIRP Test	223.0	135.0	1147.	3.53	0.502

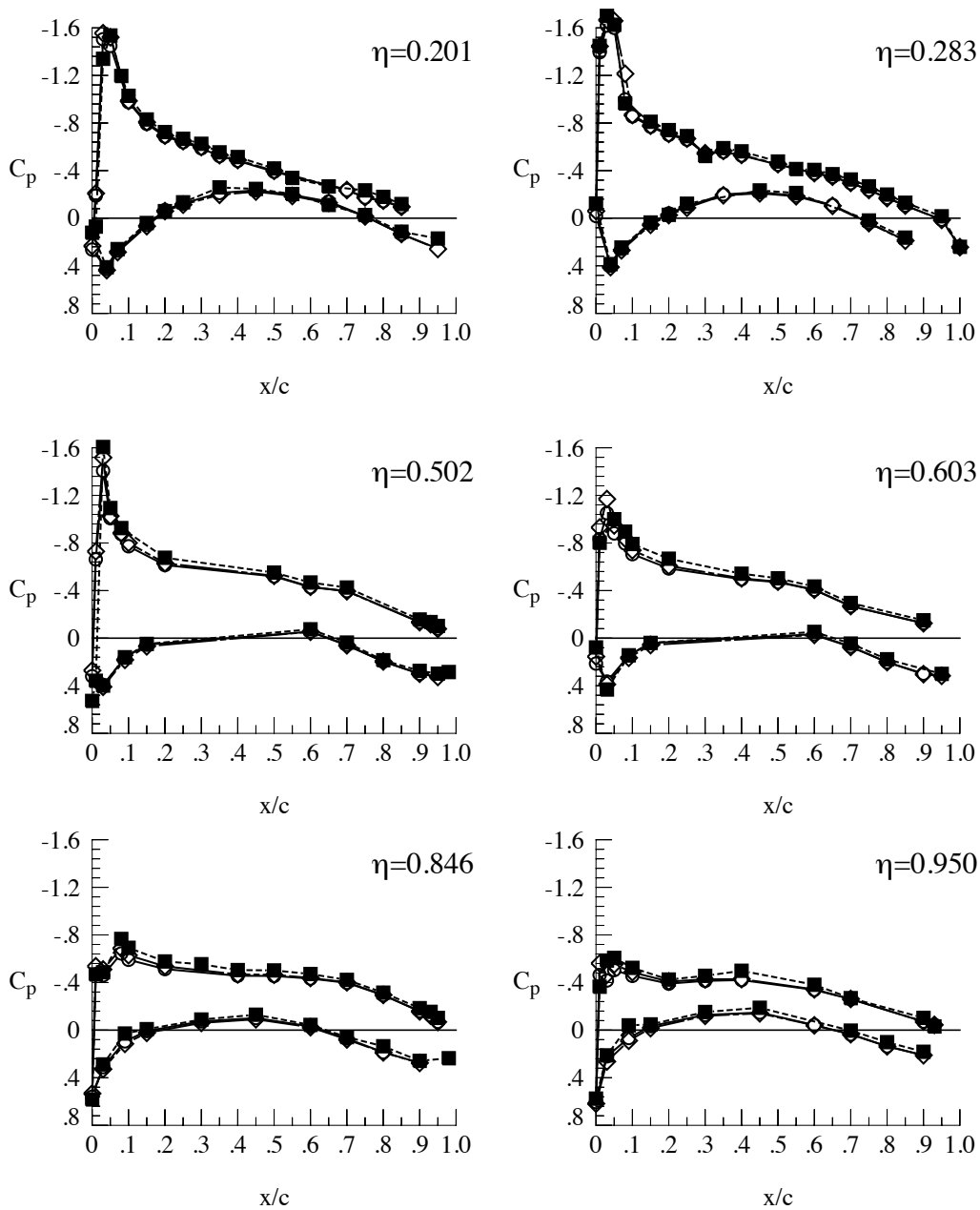


Figure 21. Surface pressures, Mach = 0.7,  $Re_c = 19.8 \times 10^6$ ,  $q_\infty = 1148$  psf.

	Facility	Run	Point	$q_\infty$ -psf	$\alpha$	$C_L$
○	ETW ESWIRP Test	226.0	110.0	1317.	2.31	0.440
■	NTF Test 197	212.0	2775.	1310.	2.63	0.470
◇	ETW ESWIRP Test	226.0	115.0	1317.	2.52	0.474

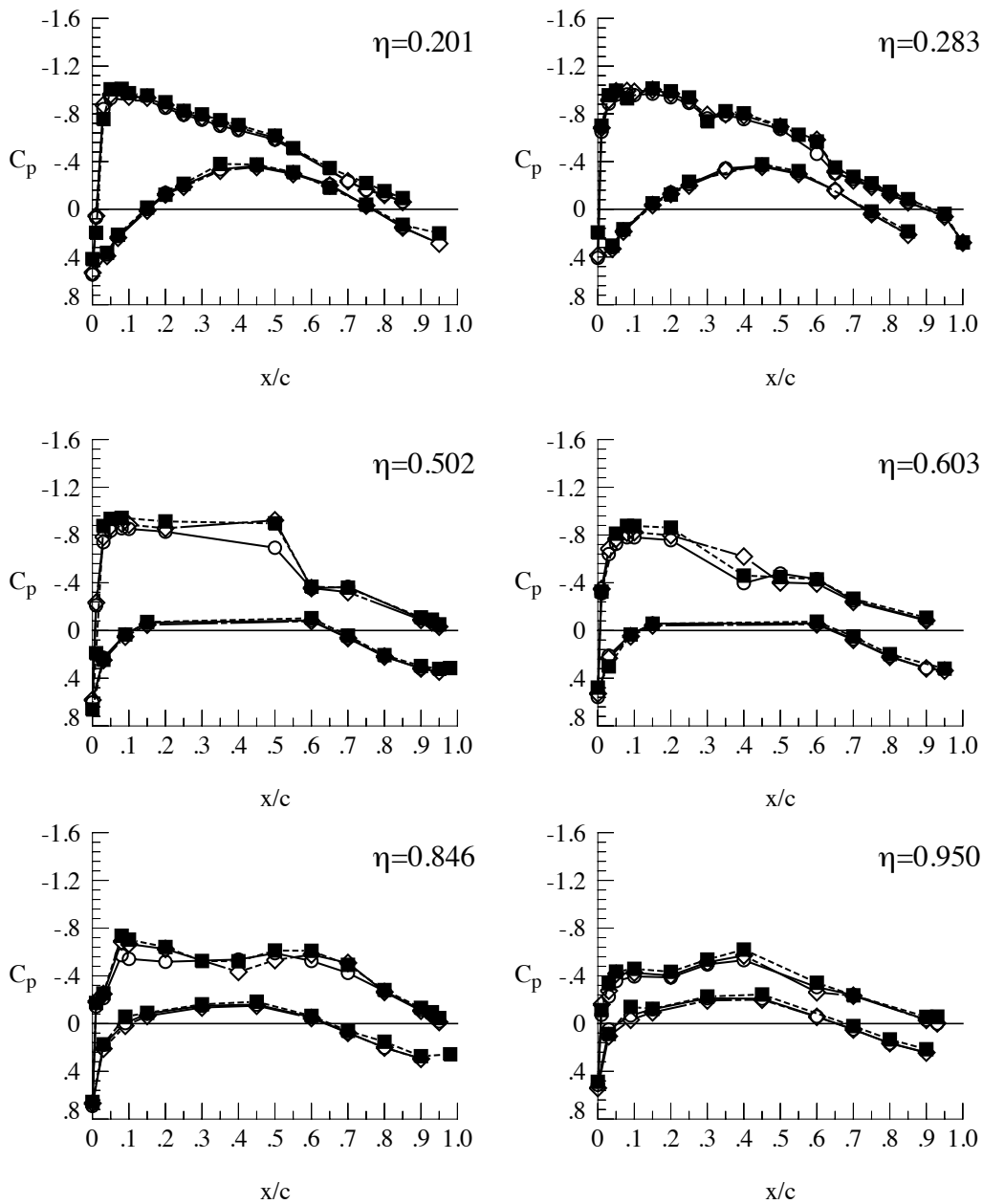
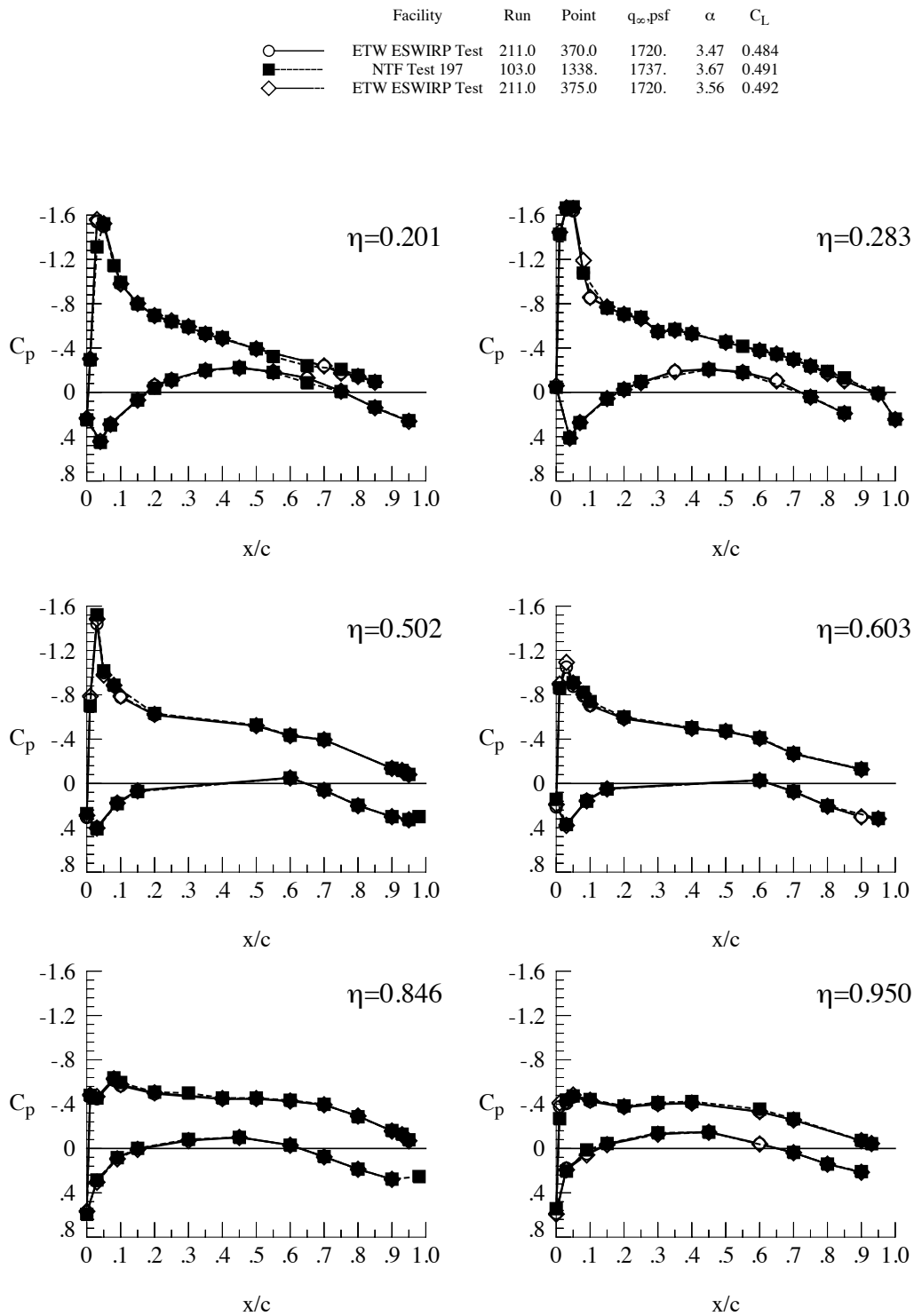


Figure 22. Surface pressures, Mach = 0.85,  $Re_c = 19.8 \times 10^6$ ,  $q_\infty = 1310$  psf.



**Figure 23. Surface pressures, Mach = 0.7,  $Re_c = 19.8 \times 10^6$ ,  $q_\infty = 1737$  psf.**

	Facility	Run	Point	$q_\infty$ ,psf	$\alpha$	$C_L$
○	ETW ESWIRP Test	213.0	265.0	1977.	2.74	0.488
■	NTF Test 197	106.0	1376.	1985.	2.91	0.493
◇	ETW ESWIRP Test	213.0	270.0	1978.	2.83	0.502

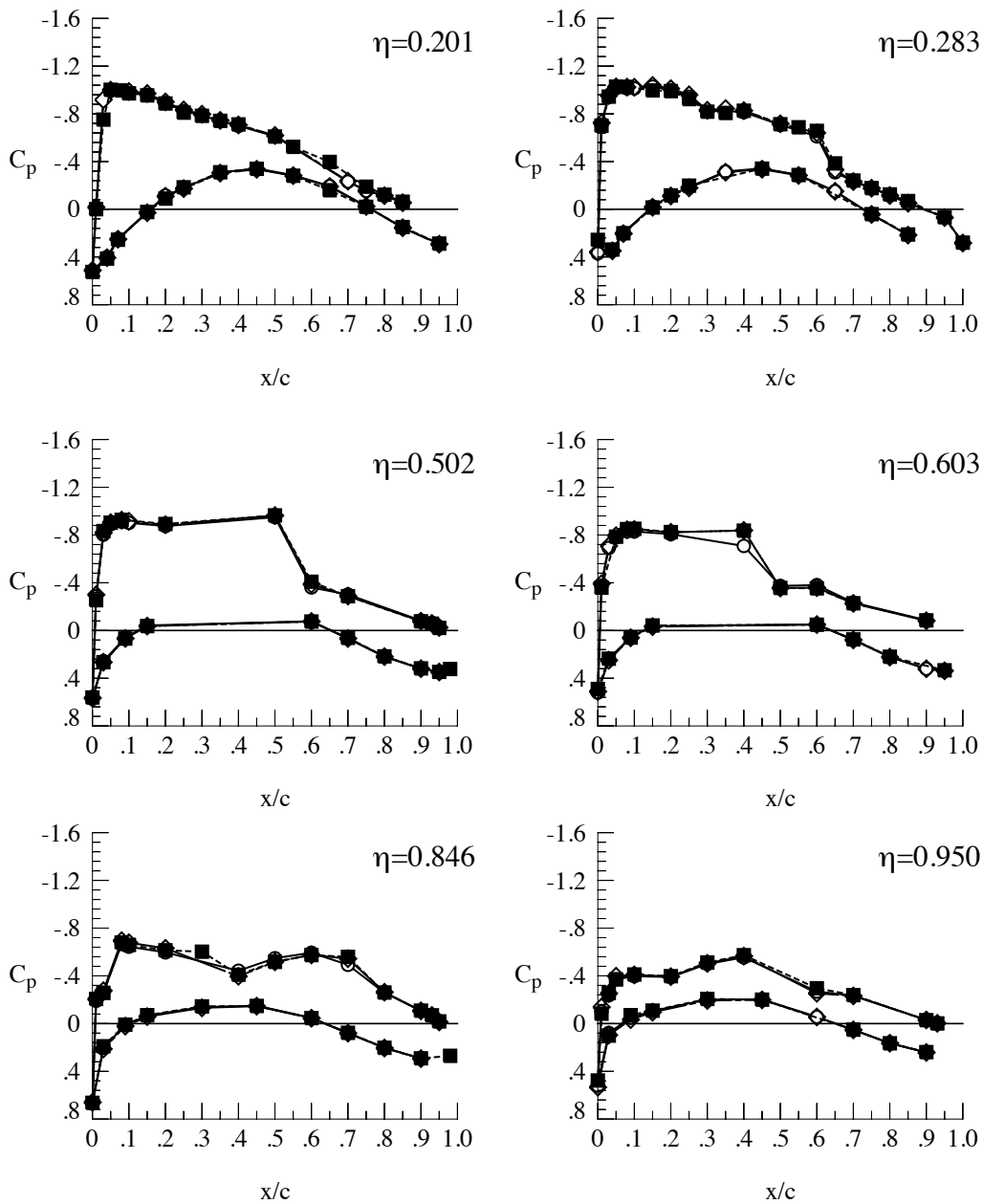


Figure 24. Surface pressures, Mach = 0.85,  $Re_c = 19.8 \times 10^6$ ,  $q_\infty = 1985$  psf.

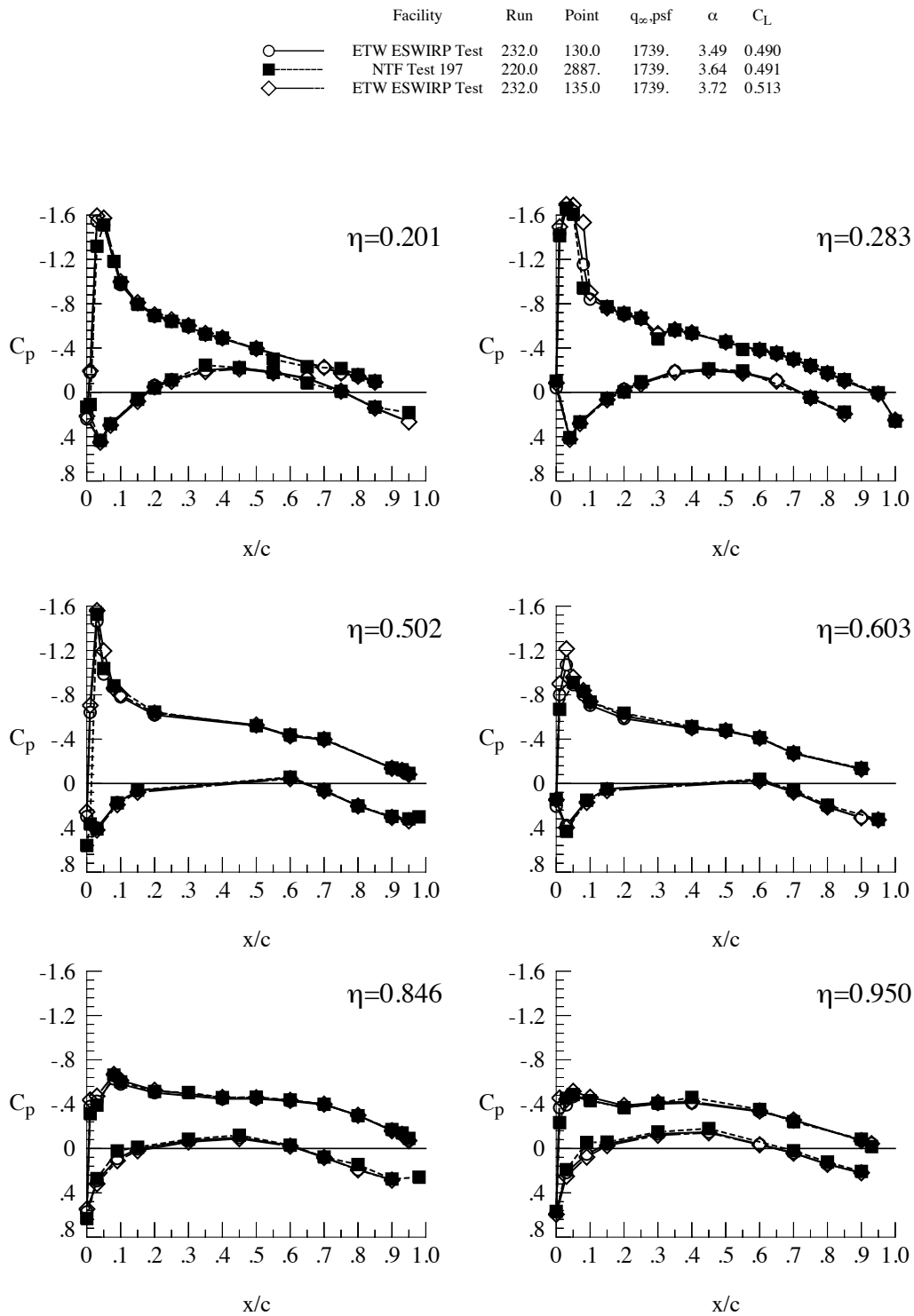


Figure 25. Surface pressures, Mach = 0.7,  $Re_c = 30 \times 10^6$ ,  $q_\infty = 1739$  psf.

	Facility	Run	Point	$q_\infty$ , psf	$\alpha$	$C_L$
○	ETW ESWIRP Test	233.0	100.0	1995.	2.33	0.434
■	NTF Test 197	223.0	2919.	1985.	2.66	0.461
◇	ETW ESWIRP Test	233.0	105.0	1995.	2.56	0.467

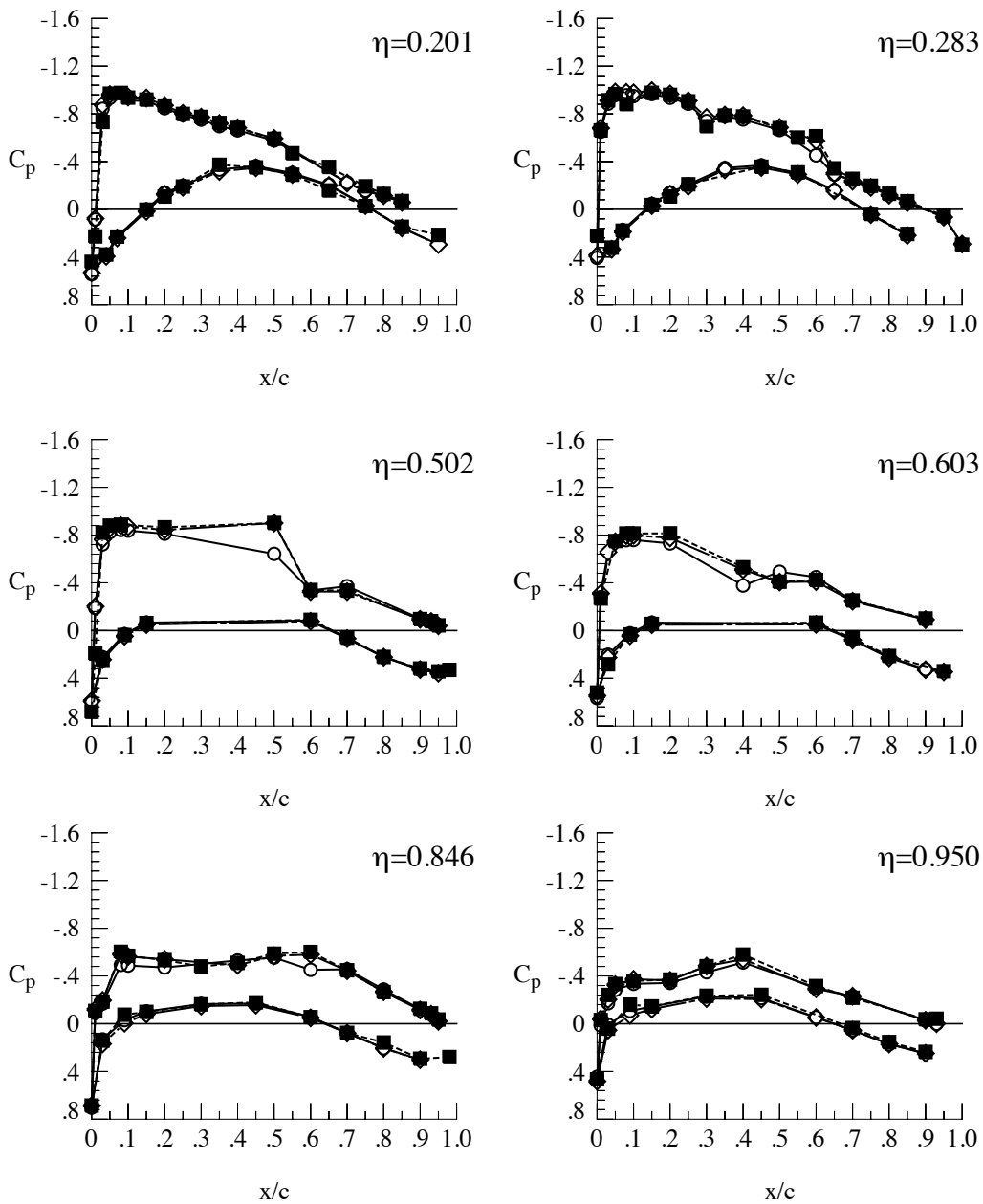


Figure 26. Surface pressures, Mach = 0.85,  $Re_c = 30 \times 10^6$ ,  $q_\infty = 1985$  psf.

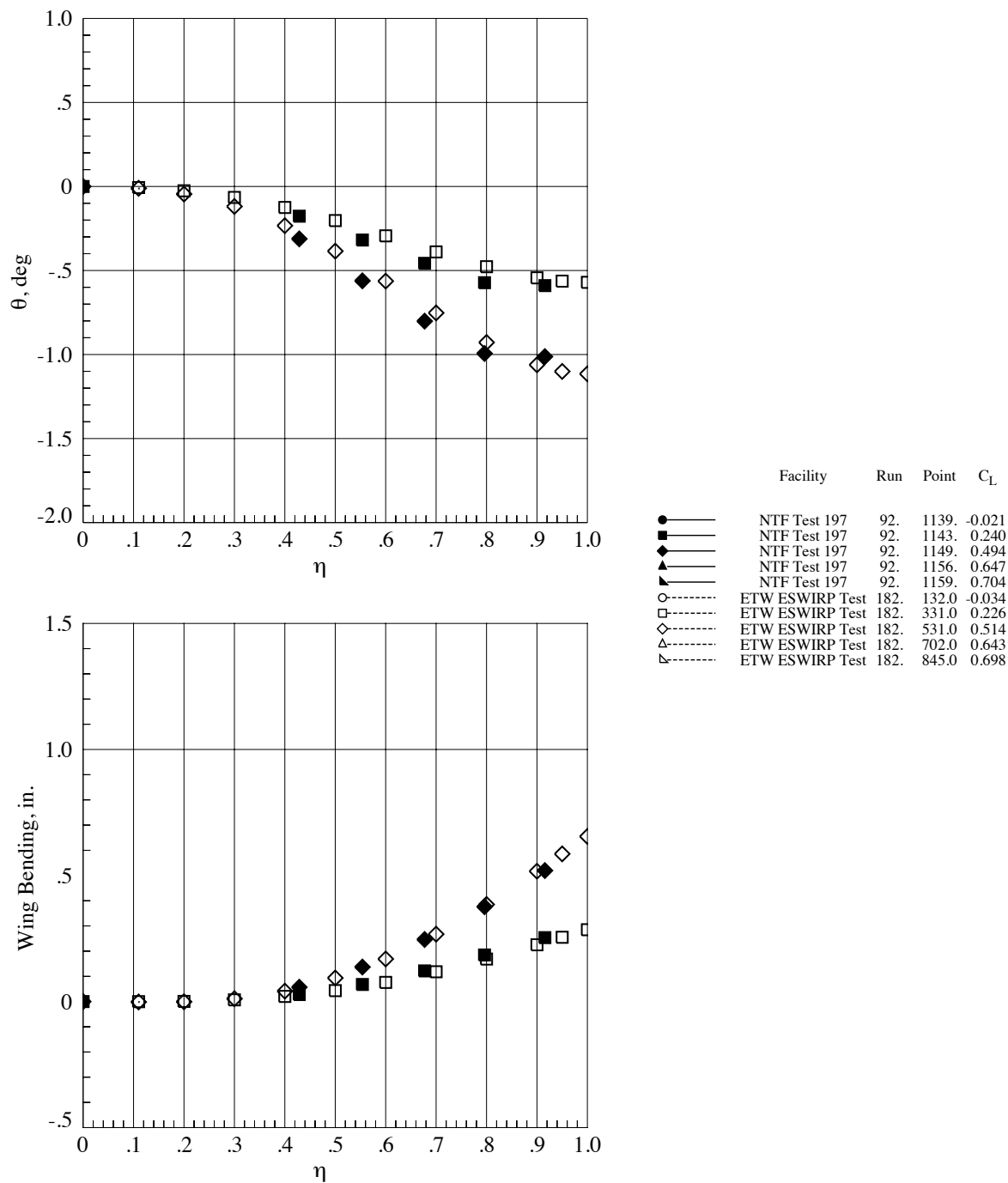


Figure 27. Wing bending and twist comparison, Mach = 0.85,  $Re_c = 5 \times 10^6$ .

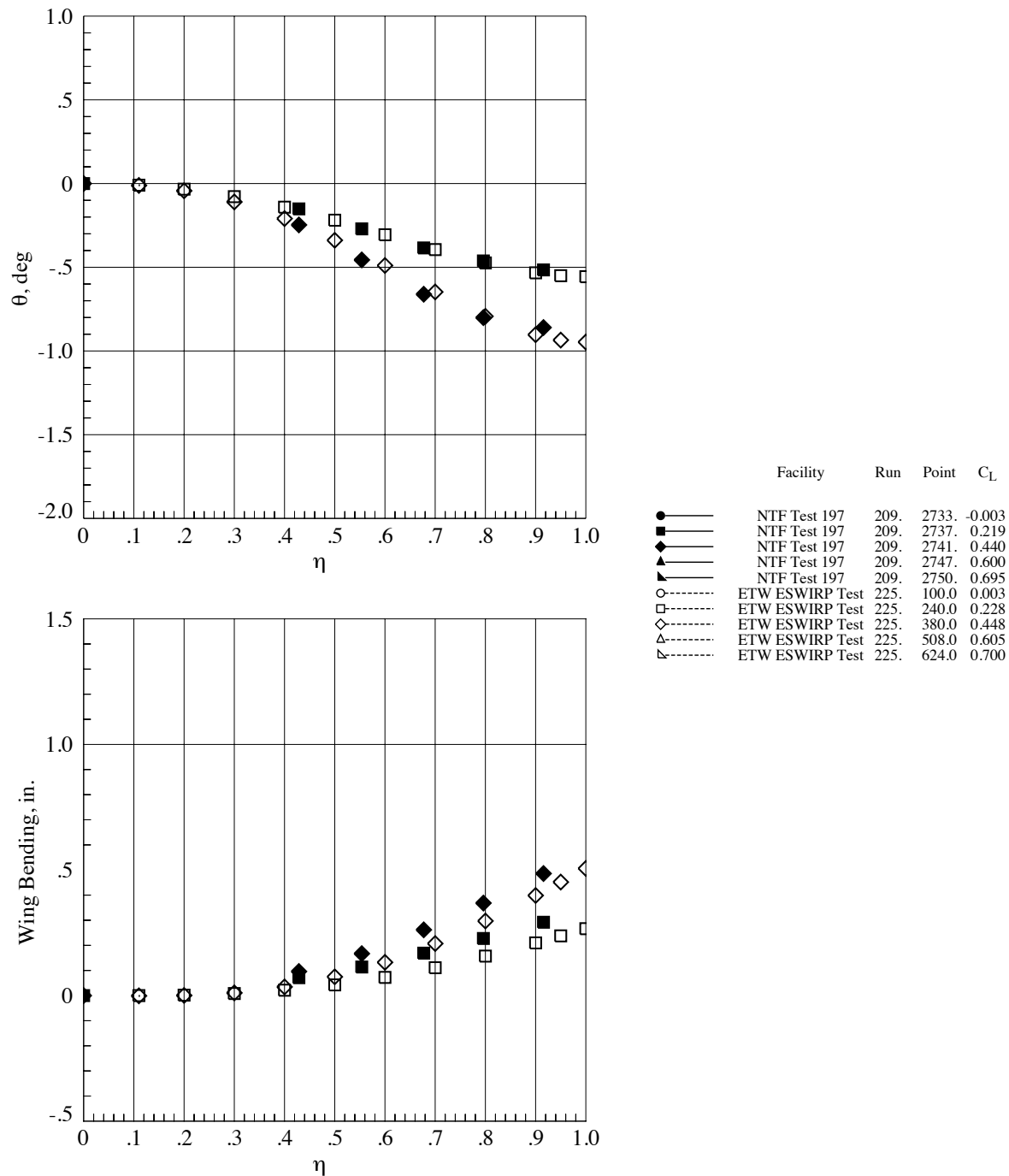
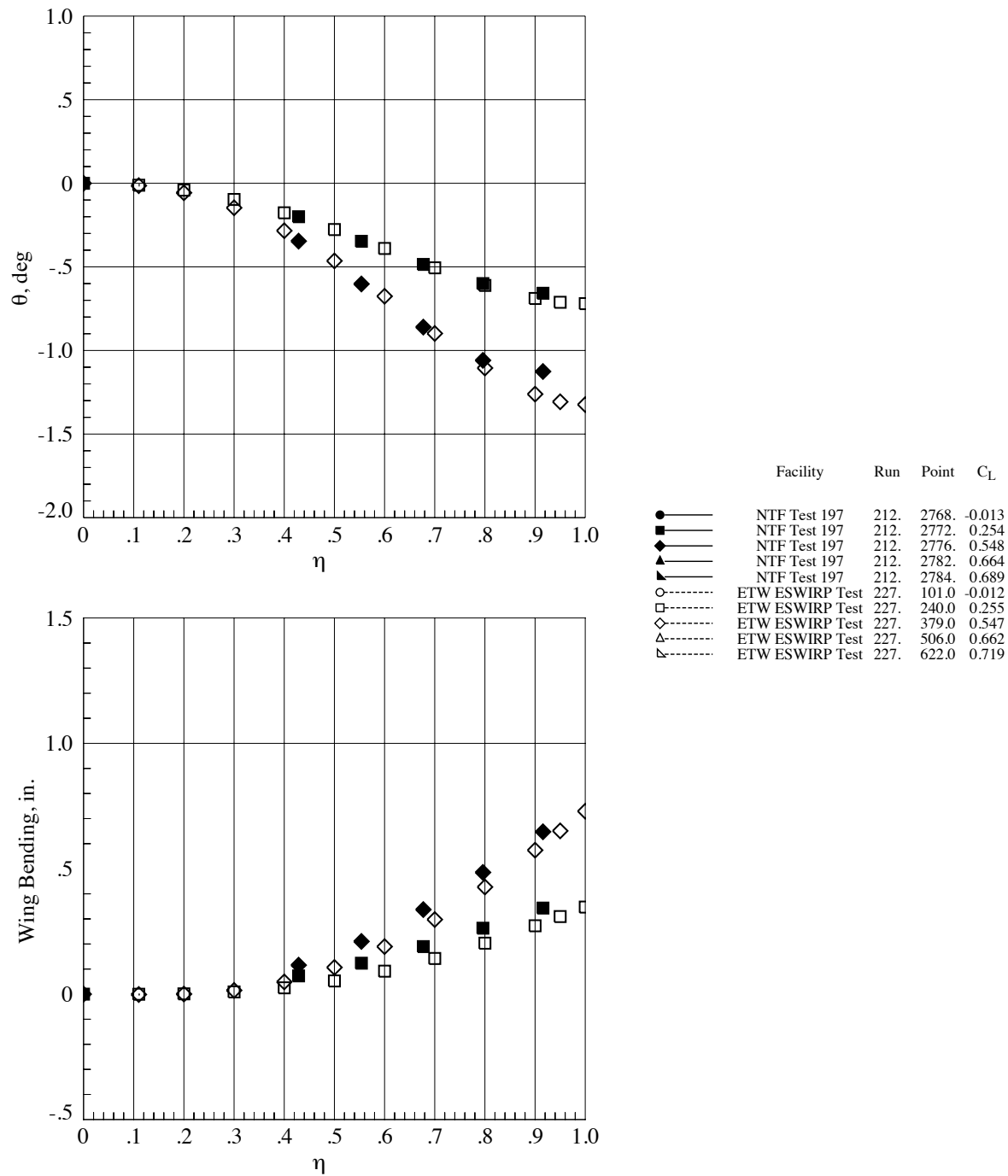
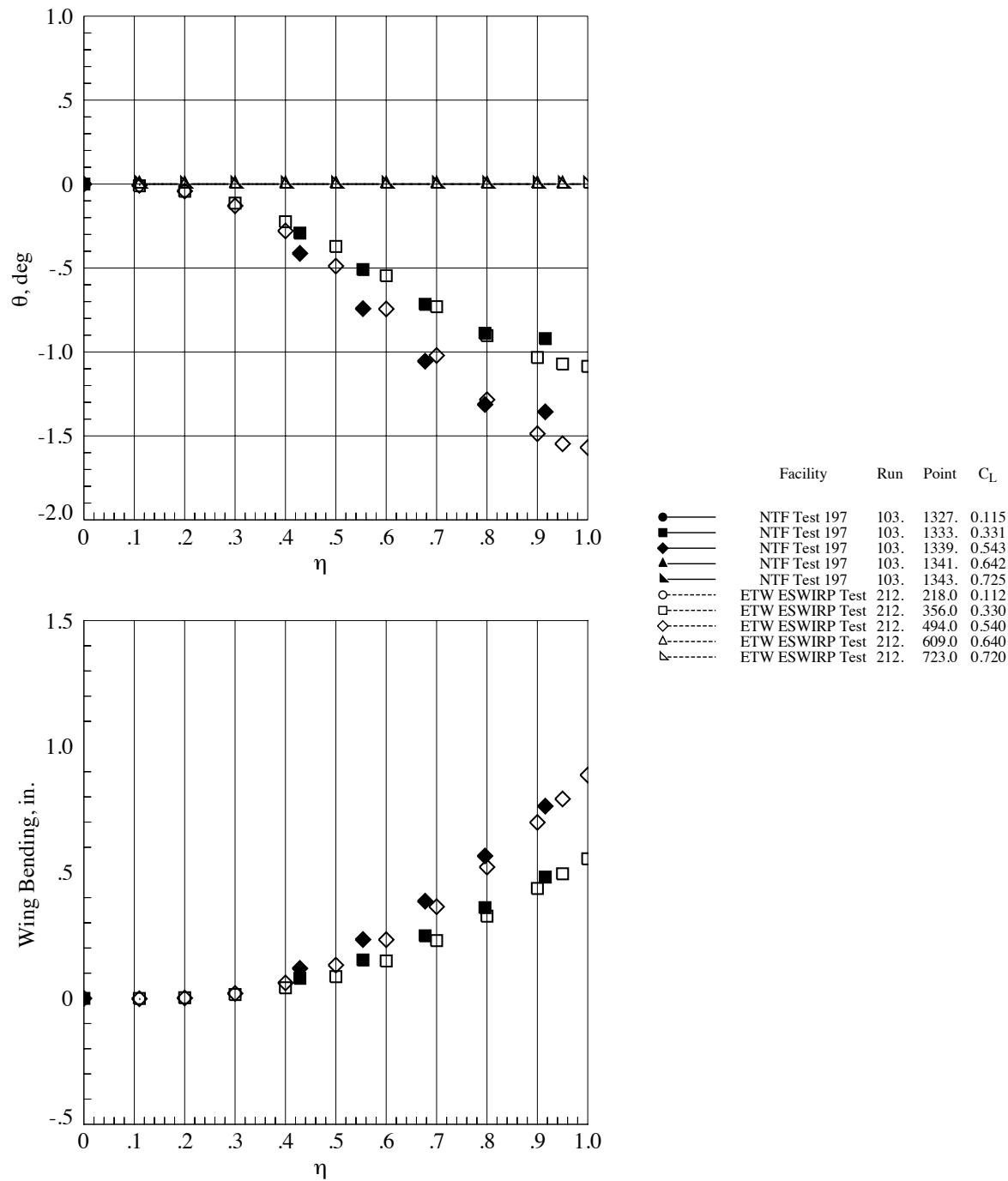


Figure 28. Wing bending and twist comparison, Mach = 0.7,  $Re_c = 19.8 \times 10^6$ ,  $q_\infty = 1148$  psf.



**Figure 29. Wing bending and twist comparison, Mach = 0.85,  $Re_c = 19.8 \times 10^6$ ,  $q_\infty = 1312$  psf.**



**Figure 30. Wing bending and twist comparison, Mach = 0.7,  $Re_c = 19.8 \times 10^6$ ,  $q_\infty = 1737$  psf.**

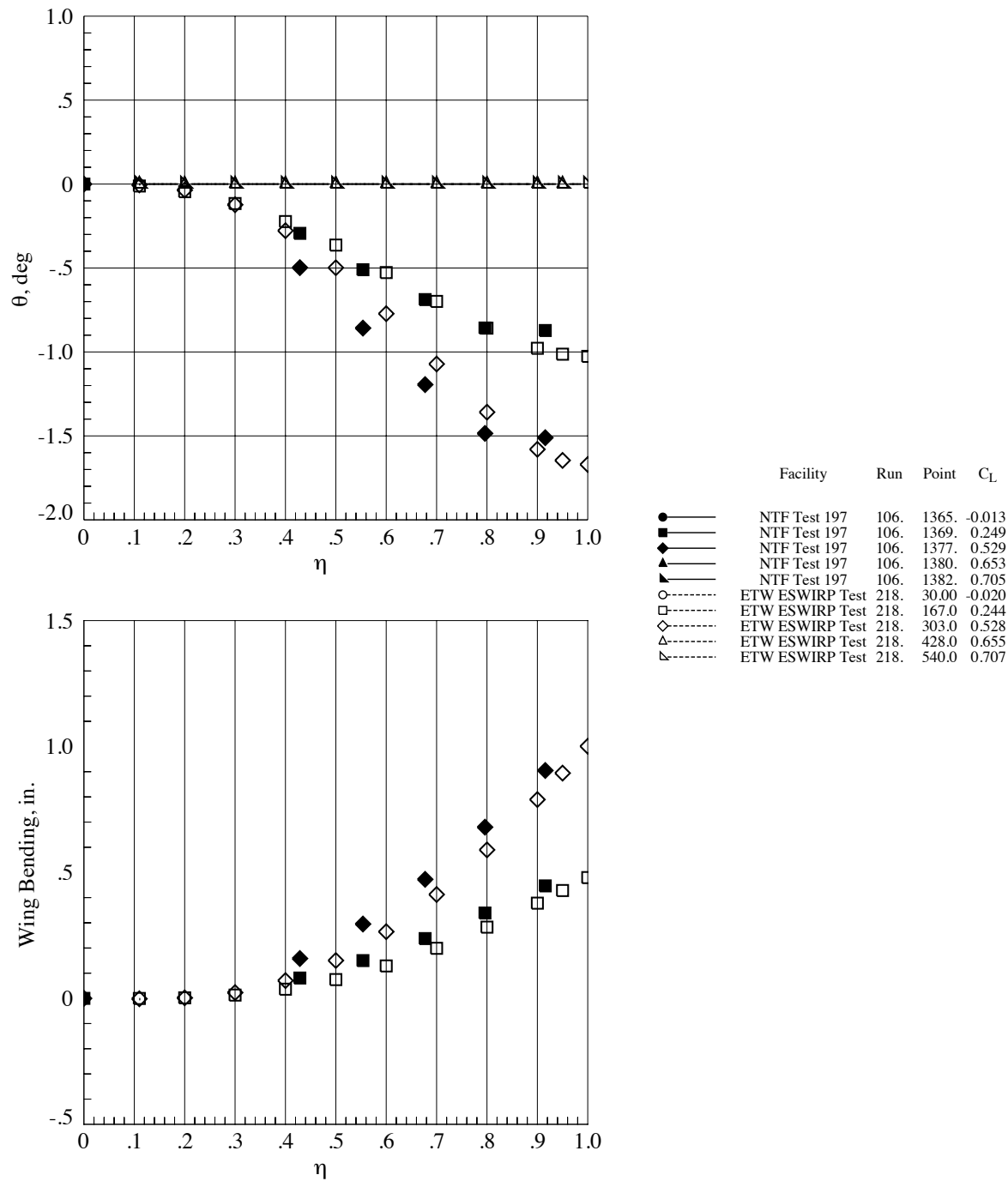


**Figure 31. Wing bending and twist comparison, Mach = 0.85,  $Re_c = 19.8 \times 10^6$ ,  $q_\infty = 1737$  psf.**

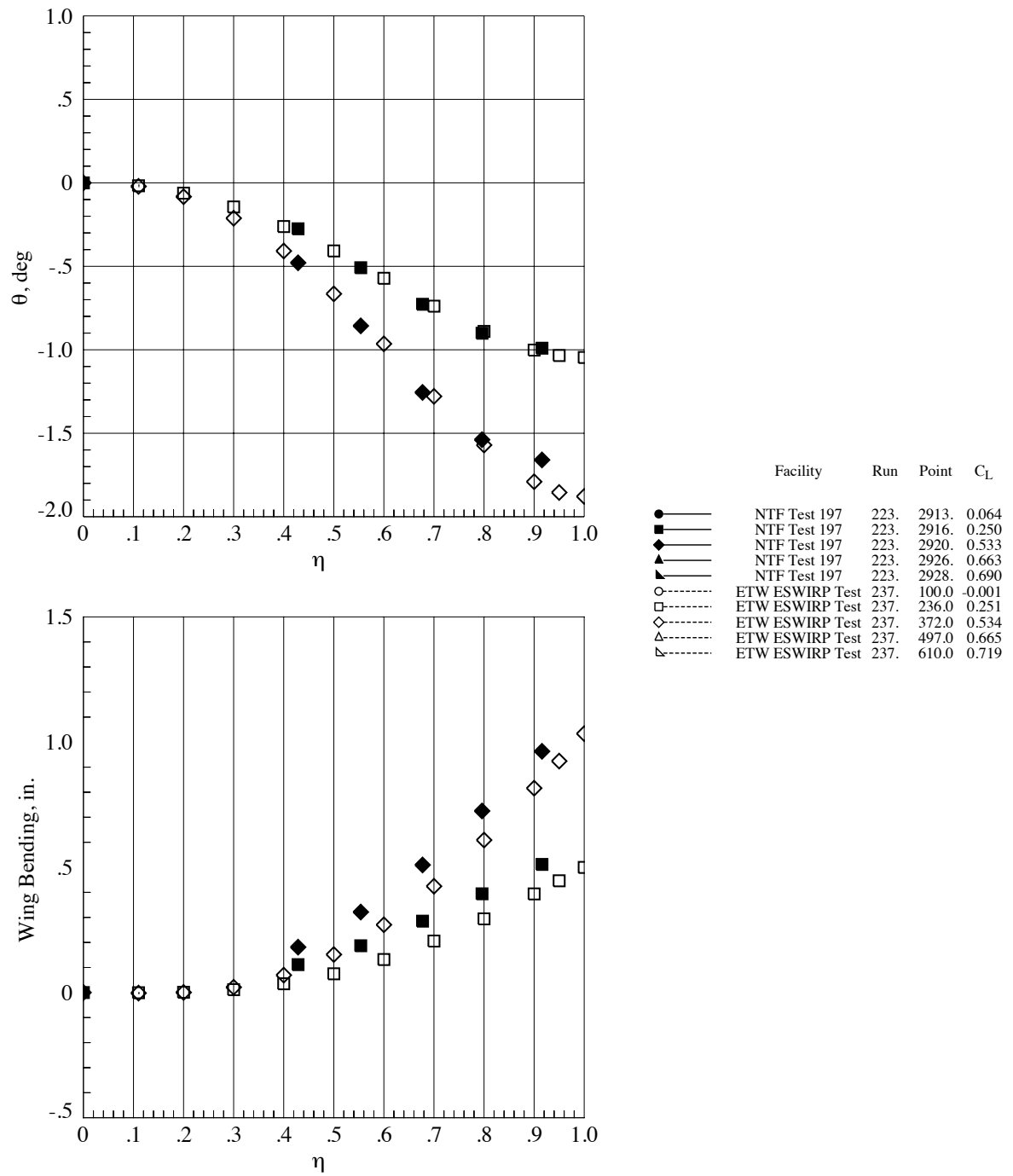


**Figure 32. Wing bending and twist comparison, Mach = 0.85,  $Re_c = 30 \times 10^6$ ,  $q_\infty = 1985$  psf.**